

**TR/02/91**

**February 1991**

**RESEARCH ON  
CONTINUOUS AND INSTANTANEOUS  
HEAVY GAS CLOUDS**

**by**

**P.C. Chatwin and G.W. Goodall**



**RESEARCH ON**  
**CONTINUOUS AND INSTANTANEOUS**  
**HEAVY GAS CLOUDS**

by

**P.C. Chatwin\* and G.W. Goodall**

*Department of Mathematics and Statistics*  
*Brunel University, Uxbridge, Middlesex, UB8 3PH.*

Final Report for the Commission of the European Communities,  
Directorate-General for Science, Research and Development, on  
Brunel University's contribution to the CEC Research Programme  
on Major Technological Hazards, Project BA: "Research on  
Continuous and Instantaneous Heavy Gas Clouds". CEC Contract  
No. EV4T.0025.UK(H).

\*Present address: Department of Applied and Computational Mathematics,  
University of Sheffield, Sheffield, S10 2UN.

February 1991

**BRUNEL UNIVERSITY**

**SEP 1991**

**LIBRARY**

w919882

## EXECUTIVE SUMMARY

This report describes the contribution of Brunel University to the joint CEC project 'Research on Continuous and Instantaneous Heavy Gas Clouds' under the Major Technological Hazards programme (CEC Contract EV4T.0025.UK(H)).

Brunel University's main task in this project was concerned with the analysis of experimental data provided by some of the other project collaborators. Liaison with these collaborators, and with others undertaking other aspects of data analysis, was obviously also important. The experimental data were obtained both from full-scale field trials (Tuv/Ris $\phi$ ) and from wind tunnel experiments (TNO, University of Hamburg, Warren Spring Laboratory). Some of the data sets are very large.

The main effort of data analysis has been concentrated on the data from Tuv/Ris $\phi$  and Warren Spring Laboratory. This was mainly because of the timely arrival of substantial quantities of data from these sources, and also to avoid direct duplication of work carried out by other collaborators. Nevertheless, some analyses were made of TNO and University of Hamburg data.

The Tuv/Ris $\phi$  data set had one extremely valuable property, namely that the concentrations were measured by several different methods. Analysis here confirmed the view - hitherto essentially a theoretical speculation with no substantial experimental support - that the instrumentation can itself have a significant effect on the measured concentration. One consequence of the results of Brunel's analysis of the Tuv/Ris $\phi$  data set is therefore that caution must be exercised in validating practical models of hazard assessment. Interest also attaches to this data set in that, in some of the experiments, obstacles were removed while the experiment was running; some analysis of "before and after" effects has been undertaken. For example, comparisons were made of such effects on levels of concentration and

(ii)

concentration variability, and two different algorithms have been developed to illustrate these features and, indeed, to determine, simply from the time series, when the obstacles were removed.

A major and most welcome feature of the Warren Spring Laboratory data set was that it recorded many repetitions of gas releases under identical experimental conditions. Because of this, it was possible to study the *variations* in the concentration data from one release to another and to build up an initial simple statistical understanding of the situation. In such circumstances, statistical measures such as mean and variance may be estimated as *ensemble averages*, rather than by considering them as time averages within a single release; this latter approach can be questionable, particularly if the data do not exhibit statistical stationarity. The results of Brunel's analysis of this data set, though not yet complete, amply justify the "repetitions" strategy. The report illustrates this conclusion by presenting typical results that could not otherwise have been obtained, and which have important implications for real-life.

The TNO wind tunnel experiments were conducted both for the purpose of comparing results with those from other wind tunnels and to provide a simulation of one of the full-scale Tuv/Risø field trials. The resulting data set is potentially very valuable, but Brunel's analysis has identified a number of points for concern. Thus there are some doubts about the behaviour of the instrumentation, while some of the experimental results are atypical of those obtained by other collaborators and occasionally seem hard to reconcile with physical intuition.

Concerning the University of Hamburg data set, Brunel was aware that extensive and detailed analyses had been carried out by the Health and Safety Executive. Brunel did not wish to essentially duplicate this effort. Brunel's work here was, therefore, largely confined to replicating some of the HSE analyses for the purpose

(iii)

of confirming results - an aim that was always achieved. The HSE analyses are discussed formally in HSE's report under this contract, and were presented informally to meetings of the collaborators during the summer.

Unavoidable resource constraints have prevented much progress in moving forward from data analysis to the development of models. However, work of this nature is still in progress after the termination of the formal contract. Such work is justified by the quantity and quality of the data, and is expected to form an important input to research under the **FLADIS** contract.





## CONTENTS

Executive Summary	(i)
1. Introduction	1
2. Theoretical Foundations	6
3. Summary of Data Analysis	11
4. Concluding Remarks	32

*Figures* following page 33



## **CHAPTER ONE: INTRODUCTION**

### **1.1 Background**

Brunel's original proposal to CEC under the Major Technological Hazards programme, written in December 1986, foresaw the employment for two years of a Research Assistant engaged (in collaboration with Professor P.C. Chatwin) on two tasks. These were (i) the analysis of data from both full-scale and model-scale trials with particular emphasis on concentration fluctuations, and (ii) the incorporation of the results from these analyses into reliable models of heavy gas dispersion with particular emphasis on practical hazard assessment. An important part of the Brunel contribution was expected to be liaison with all other project collaborators, particularly those also undertaking data analysis.

In the event there were two major developments which necessitated changes to the programme of work at Brunel that was originally proposed. First, the proposal was successful but only at a reduced funding level (50 kECU instead of 85 kECU). Thus the final research programme (Annex I of the Contract with CEC dated 2 October 1987) could only allow 1 man-year's effort on data analysis and model development. In the event, and following consultation with Dr. P.D. Storey (MTH Programme Coordinator) and other appropriate CEC personnel, it was decided that Brunel's contribution to the overall programme could be maximised - in terms of both quality and quantity of achieved results - by employing two of its own students, each for the 6 month period from April to September 1990, as part of the Industrial Training work programme that each Brunel undergraduate is required to undertake as an integral part of the degree course. Two of the reasons for this decision were the consequent minimisation of the time needed for familiarisation with Brunel's computing organisation and other administrative arrangements, and the abolition of the time (and costs) involved in recruiting and rehousing a Research Assistant from outside. (Relevant also was the recognition that it was likely to be very difficult to

hire a person with the requisite ability, energy and qualifications for a period of only 1 year.) This important decision proved, in our opinion, to be the correct one. The students involved were Mr. P. Burge and Mr. S.P. Decent; they worked under the day-to-day supervision of Professor Chatwin and, especially, his colleague Mr. G.W. Goodall. Mr. Goodall also carried out substantial data analysis himself. Valuable advice and assistance was often provided by Dr. N. Mole, another staff member at Brunel working full-time on another project in a closely-related area sponsored by the UK Ministry of Defence. The second major development, in most ways a very welcome one, was that the quantity and the quality of the data collected by our collaborators involved in conducting experiments (TuV/Risø-field; TNO, UH, WSL - wind tunnels) were much greater than had been anticipated, and much too great to allow anything like a comprehensive analysis. Consequently the data analysts in the project, including Brunel, had to take decisions (and rapidly so in Brunel's case because of the short duration of the time period during which data analysis had been scheduled, and because of some delays in receiving validated data tapes and diskettes from two of the experimental groups) about priorities. The particular decisions taken are stated and justified in the relevant places in the body of this report.

It is appropriate to record here however that these developments, and the decisions taken in response to them, resulted in there being much data that have either not been analysed or not to the extent that are merited (or were originally envisaged). Nor has it been possible to carry forward the model development (with testing and validation against the data) to any significant extent. Fortunately it is expected at the time of this writing that almost all the collaborators on Project BA will be involved in a follow-up project under the CEC STEP programme (FLADIS) in which it will be appropriate to complete these tasks and to extend the results from the near-field (as emphasised by Project BA) to the far-field (as emphasised by FLADIS). This use of the Project BA data in the FLADIS project has been an

explicit part of the successful proposals under the STEP programme application.

## **1.2 Associated developments**

During the period of the project (01/01/88 - 31/12/90) other work and activities at Brunel (and elsewhere) have continued on closely related themes. As already noted, this period overlapped with work supported by the UK Ministry of Defence (Dr. Mole and Dr. N.T. Hajian), and some of the results obtained will be described later when relevant. Professor Chatwin's longstanding collaboration with Professor P.J. Sullivan of the University of Western Ontario, London, Canada continued and resulted in several theoretical developments believed to be highly relevant to the objectives of the MTH programme, particularly Project BA. Professor Chatwin gave lecture courses on turbulent diffusion/atmospheric dispersion at the von Karman Institute for Fluid Dynamics (1989) and ICTP, Trieste (1990). Many Project BA collaborators attended specialised conferences on concentration fluctuations at Brunel organised by Professor Chatwin under the auspices of EURASAP (April 1988) and EUROMECH (September 1989).

## **1.3 Plan of the report**

Chapter Two summarises the theoretical framework underpinning the original proposal and the work performed at Brunel under the project, with emphasis on the most recent developments. Chapter Three is a relatively concise summary of the results of the data analyses. No attempt has been made to include all the results obtained since this would be practically impossible (space and time) and would not direct attention to what are believed to be the most important findings. Nor have software listings been given. Full details of the latter, as well as other results, can be obtained by writing to Professor Chatwin. The final Chapter of the report presents conclusions and recommendations.

#### 1.4 Relevant publications

Apart from Project BA progress reports, the following written material has been produced during the contract period by Professor Chatwin and his colleagues.

- K.K. Carn, S.J. Sherrell and P.C. Chatwin 1988 *Analysis of Thorney Island data: variability and box models*. In **Stably Stratified Flow and Dense Gas Dispersion** (edited by J.S. Puttock, OUP), 205-231.
- N. Mole 1989a *Estimating statistics of concentration fluctuations from dispersion data*. **Proc. 4th Int. Workshop on Wind and Water Tunnel Modelling of Atmospheric Flow and Dispersion**, Karlsruhe.
- P.C. Chatwin, N.T. Hajian, N. Mole and C.D. Jones 1989 *Investigations on the atmospheric dispersion of clouds containing charged tracers*. **IMA Journal of Applied Mathematics** **42**, 97-117.
- P.C. Chatwin 1989 *Scalar transport in turbulent shear flows*. **Lecture Series 1989-03 (Turbulent Shear Flows)**, von Karman Institute for Fluid Dynamics, Rhode-St-Genève, Belgium, pp.71.
- P.C. Chatwin and P.J. Sullivan 1989a *The intermittency factor of scalars in turbulence*. **Phys. Fluids A1**, 761-763.
- P.C. Chatwin and P.J. Sullivan 1989b *The intermittency factor of dispersing scalars in turbulent shear flows. Some applications of a new definition*. **Proc. 7th Symp. On Turbulent Shear Flows**, Stanford, CA, 29.4.1 - 29.4.6.
- N. Mole 1989b *Estimating statistics of concentration fluctuations from measurements*. **Proc. 7th Symp. on Turbulent Shear Flows**, Stanford, CA, 29.5.1 - 29.5.6.
- P.C. Chatwin and P.J. Sullivan 1990a *A simple and unifying physical interpretation of scalar fluctuation measurements from many turbulent shear flows*. **J. Fluid Mech.** **212**, 533-556.
- P.C. Chatwin and P.J. Sullivan 1990b *Cloud-average concentration statistics*. **Maths. and Computers in Simulation** **32**, 49-57.

- N. Mole 1990 *A model of instrument smoothing and thresholding in measurements of turbulent dispersion*. **Atmos. Envir. 24A**, 1313-1323.
- P.C. Chatwin and N.T. Hajian 1990 *Concentration fluctuations in atmospheric dispersion*. **Report to Chemical Defence Establishment**, pp.54.
- P.C. Chatwin 1990 *Air pollution modelling for environmental impact assessment*. **Lectures given at ICTP, Trieste**, pp.25.

## CHAPTER TWO: THEORETICAL FOUNDATIONS

### 2.1 Concentration fluctuations and the pdf of concentration

In any release of a contaminant into a turbulent flow, such as that in the atmosphere, the concentration  $\Gamma$  of the contaminant (in arbitrary units) is a random variable. This applies irrespective of the nature of the contaminant, but it often happens that the contaminant itself has significant effects on the turbulent flow. In particular, this occurs (through buoyancy forces) when heavy gases are released into the atmosphere, and the data obtained and analysed during Project BA were all from experiments of this type (as were the trials some years ago at Thorney Island).

Since  $\Gamma$  is a random variable, its proper scientific description must be a statistical one. In respect to a well-defined ensemble (or population) of releases, this means a full description requires an infinite set of probability density functions (referring to the values of  $\Gamma$  at all possible sets of points and times). The investigation of this full description is in its (early) infancy and the only probability density function (henceforth abbreviated to pdf) whose properties are currently being studied to any significant degree is the simplest, namely  $p(\theta; x, t)$ , where  $x, t$  denote position and time respectively, and, in accordance with standard practice,

$$p(\theta; x, t) = \frac{d}{d\theta} \{ \text{prob}[\Gamma(x, t) \leq \theta] \} \quad (1)$$

Equation (1) holds for all  $\theta$  satisfying  $0 < \theta \leq \theta_{\max}$  where  $\theta_{\max} = \theta_{\max}(x, t)$  is the highest possible concentration. (It is - of course - not the highest concentration observed in any one release.) Thus  $p(\theta; x, t) = 0$  for all  $\theta > \theta_{\max}$ ; since  $\theta_{\max}$  is in general unknown it is simplest to take the domain of  $p(\theta; x, t)$  as  $(0, \infty)$ . It follows from (1) that

$$p(\theta; x, t) = \text{prob}[\theta < \Gamma(x, t) < \theta + \delta\theta] \quad (2)$$

for any small positive  $\delta\theta$ , and (2) probably provides a more useful interpretation of the pdf.

There are several important basic properties of  $p(\theta; x, t)$ . First, since it is a pdf,



$$\int_0^{\infty} p(\theta;x,t)d\theta = 1. \quad (3)$$

Secondly, the mean  $\mu(x,t)$  and the variance  $\sigma^2(x,t)$  of the concentration are defined in the standard manner by

$$\mu(x,t) = \int_0^{\infty} \theta p(\theta;x,t)d\theta; \quad (4)$$

$$\sigma^2(x,t) = \int_0^{\infty} [\theta - \mu(x,t)]^2 p(\theta;x,t)d\theta = \int_0^{\infty} \theta^2 p(\theta;x,t)d\theta - \mu^2(x,t). \quad (5)$$

It is perhaps appropriate to make one or two comments about notation. That used in this report, including the symbols for mean and variance, is (more or less) conventional for statistics. It has not been conventional in turbulent diffusion (including atmospheric dispersion). However the conventional statistical notation is rather neater (no dashes and overbars) and even more widely known. Moreover the standard use of the overbar in turbulent diffusion - to denote a population mean - is inconsistent with its standard use in statistics - to denote a sample mean. (Thus more conventional notation until now would have been to write  $\Gamma = C + c$  or  $\Gamma = \bar{\Gamma} + c'$ , where  $C$  and  $\bar{\Gamma}$  are the same and equal to the quantity  $\mu$  defined in (4), and  $c$  and  $c'$  are also the same and denote the concentration fluctuation. The quantity  $\sigma^2$ , defined in (5), has more conventionally been denoted by  $\overline{c^2}$  or  $\overline{c'^2}$ , and is normally termed the mean square fluctuation.)

Irrespective of notation, it is essential to note that the mean concentration  $\mu(x,t)$  is **not** a time average, unless conditions are statistically stationary. Statistical stationarity can occur only when the contaminant is released continuously at a steady rate into an atmosphere in which the turbulence is also statistically stationary. The former of these conditions was not satisfied in any of the series of experiments considered in this report (although it could have been regarded as being approximately met in some of them and - indeed - it was convenient to make this assumption for some analyses). When conditions are not statistically stationary, statistical properties like  $\mu$ ,  $\sigma^2$  and  $p(\theta;x,t)$  can be estimated only by appropriate averages (usually arithmetical) over the results of many repetitions of an experiment. In the past, turbulent diffusion and atmospheric dispersion research almost

exclusively emphasised the mean concentration  $\mu$ . One consequence of this has been the development of models for air quality and hazard assessment expressed entirely in terms of  $\mu$ , or more precisely (and unjustifiably in view of the previous paragraph) in terms of time-average concentrations. Apart from being scientifically wrong and unrealistic - even the most casual observation of any dispersing contaminant, e.g. smoke from a chimney, shows that the structure of the concentration field does not have the smoothly varying behaviour of  $\mu(x,t)$  - such models are not even practically adequate, at least in the cases that have been investigated in any detail. One of these is the assessment of the hazard of flammability. Work by Birch, Brown and Dodson of British Gas has shown conclusively that serious errors of assessment will arise if only the mean concentration is considered and, moreover, that satisfactory assessments of ignitability are obtained by using  $p(\theta;x,t)$ . For the case of toxic gases, Griffiths and Ride have illustrated that large underestimates of casualties are obtained if assessment is based only on average concentrations or dosages.

For such reasons existing models for controlling air quality and for assessing hazards associated with dispersing gases (including heavy gases) must be replaced by a new generation of models which, to reflect both scientific correctness and real needs, must be statistical. Much research is needed to establish and validate such models, and the work under Project BA has made, and will make, an important contribution to this aim.

## 2.2 Some recent research results on statistical properties of $\Gamma$

Apart from the mean concentration  $\mu(x,t)$ , the simplest statistical properties of the concentration field are the variance  $\sigma^2(x,t)$  and the pdf  $p(\theta;x,t)$ , and much fuller knowledge of these, including of course their dependence on release conditions (such as source type and size, initial density, ....) and the ambient atmospheric turbulence, is obviously essential if the new generation of models is to be established satisfactorily. Although exact equations for  $\mu$ ,  $\sigma^2$  and  $p(\theta;x,t)$  can easily be obtained from the standard mass conservation equation for  $\Gamma$ , these equations exhibit the insuperable difficulties caused by the closure problem (which are much more severe for heavy gases than for passive tracers). While limited progress has been made by "direct attacks" on these equations, other lines of research would seem to be more

promising at the moment. Chief among these is the analysis of high quality data within a theoretical framework that is statistical, and scientifically correct. Only within such a framework can the results of experiments be used with any confidence in constructing models.

One practically sensible research area that is receiving much attention is the investigation of whether simple two- or three-parameter models (e.g. lognormal, truncated Normal, gamma, Weibull, ...) of  $p(\theta;x,t)$  can adequately describe real circumstances and, if so, under what restrictions. For example, Chatwin and Sullivan have shown that an exact representation of  $p(\theta;x,t)$  is given by

$$p(\theta;x,t) = \gamma(x, t) = f(\theta; x, t) + [1 - \gamma(x, t)]g(\theta; x, t), \quad (6)$$

where  $\gamma$  is an intermittency factor and  $f$  and  $g$  are themselves pdfs. In practice  $\gamma$  is often much less than 1, and it is sufficient to restrict attention to  $g$  and, in particular, to ask whether one of the relatively simple distributions mentioned above can approximate it adequately.

This is a popular research field, and different research groups have their own favoured candidates! Undoubtedly the situation will clarify in due course but not until greater attention has been paid, both experimentally and theoretically, to several important influences that the instruments used to measure the concentration  $I$  can have on the estimation of the most appropriate simple model for  $p(\theta;x,t)$ . Included among such influences are inherent spatial and temporal averaging, thresholding and the influence of noise. (The last two are especially important in the frequent practical circumstances, such as those arising from toxic hazards, that require acceptably accurate estimates of highly probable and dangerous, but low, concentrations.) Mole has done important work in this area and the analysis of one of the datasets in Chapter Three highlights its (potential) importance.

Another recent result has been obtained for statistically stationary flows by Chatwin and Sullivan by analysing many datasets. This is that  $\mu$  and  $\sigma^2$  are simply related to good approximation by the equation

$$\sigma^2 = \beta\mu(\alpha\mu_0 - \mu) , \quad (7)$$

where  $\alpha$  and  $\beta$  are constants, and  $\mu_0$  is the maximum value of  $\mu(x)$ . This relationship has a simple and robust physical origin which suggests that it could be relevant to statistically unsteady dispersion, as in most atmospheric dispersion scenarios. Unfortunately there have not been any measurements of  $\mu(x,t)$  and  $\sigma^2(x,t)$  in such circumstances.

### **2.3 Conclusion**

For reasons of space this Chapter has provided only a very brief (and selective) summary. Further details can be found in the papers listed in §1.4, and in the references cited in those papers.

## **CHAPTER THREE: SUMMARY OF DATA ANALYSIS**

### **3.1 Introduction**

For the reasons given in §1.1, data were analysed at Brunel only during the period from April to September 1990. At the beginning of April, data were available from all four series of experiments (TuV/Risø; TNO; UH; WSL). Of these, the tape from TNO could not at that stage be read by either Brunel or HSE, and enquiries were being made about the causes; a data set on discs was made available by the end of April. Dr. J.K.W. Davies of HSE had already undertaken some analyses of the UH data; these were presented and discussed at a meeting at Brunel on 24 April 1990. At the meeting, chaired by Professor Dr. P.J.H. Bultjes of TNO and involving representatives from Brunel, HSE, TNO and WSL, the problem of data availability and the overall data analysis strategy were considered. In view of Dr. Davies' work on the UH data, it was subsequently decided that Brunel, in the person of Mr. Goodall, would perform only some spot checks on these data. These confirmed Dr. Davies' analysis. Mr. Goodall's main analysis would be of the TNO data, and this took place later in the summer. The two largest datasets available at Brunel at the beginning of April 1990 were from TuV/Risø and WSL; accordingly the bulk of its effort was directed to these.

Subject to the supervision arrangements described in §1.1, these datasets were analysed by Mr. Burge (WSL) and Mr. Decent (TuV/Risø). In general terms, the aim of each analysis effort was to extract as much useful information as possible of relevance to subsequent model construction and validation. Given the great differences between the two sets of trials and the type of data obtained, it was necessary for Professor Chatwin and Mr. Goodall to take separate decisions for each analysis on almost a daily basis. Preliminary accounts of the results obtained were presented at a meeting at Risø on 28-29 August 1990 involving all Project BA participants, and at the Plenary Meeting of all MTH programme contractors in Brussels on 11 October 1990. Additionally there was, of course, frequent consultation throughout the summer with many Project BA collaborators, especially HSE, Risø and WSL.

As explained in §1.3, the remainder of this Chapter is not a comprehensive account of all the results of Brunel's analysis, but a selective summary of the most important findings. In all cases, however, care has been exercised to ensure that the results are typical of the datasets.

### 3.2 Data from TuV/Risø

If necessary, reference should be made to companion reports by TuV and Risø for full details of these experiments, of the several methods used for measuring the concentration  $\Gamma$  of gaseous propane, and of the data acquisition and storage systems. In preparing the present account, reference has been made to earlier papers whose authors include Dr. M. Heinrich of TuV and Drs. N.O. Jensen and M. Nielsen of Risø; particular help was provided by Dr. Nielsen's draft report *Preliminary Treatment of Meteorological Data from Project BA Dense Gas Experiments, Risø-M-2882*, dated July 1990.

The trials all took place on flat terrain on a site at Lathen in NW Germany with liquid propane being released from two types of source: jet (with momentum) and cyclone (no net momentum). In many of the experiments (including all those analysed at Brunel), obstacles were present in the field in the form of 2m high "walls" (some solid and some 50% porous); in most cases one (or more) of the walls was removed during the experiment, usually about half-way through. The releases were at a constant rate for periods of order 5 min for the experiments analysed at Brunel. None of the experiments was a repeat of another, nor was this intended.

Consequently, estimates of statistical properties of  $\Gamma$  could be made only by regarding suitable segments of its time series as approximately records of statistically stationary releases (see §2.1). Moreover, given that obstacles were removed during the experiments, the lengths of such records were effectively only of order 2 min, and experience (see e.g. the report by Chatwin and Hajian (1990) referenced in §1.4) suggests that this is much too short to obtain statistically stable estimates of parameters like  $\sigma^2$  and  $p(\theta; x, t)$ . In these circumstances, and given that Brunel's contract emphasised the variability in  $\Gamma$  (concentration fluctuations), it was decided to put most effort into exploiting one of the most unusual and valuable

features of the trials, namely the existence for some masts in some trials of 4 different measurements of  $r$ .

Reference has been made in §2.2 to the large influence on perceived concentrations of the instruments used to measure them. To measure  $r$ , the TuV team used about 30 catalytic type gas detectors with a response time of about 5-10s, but recorded on diskettes at 1.25Hz. (They also used a smaller number of infra-red and cuvette type devices; although Brunel has also analysed data from these to a limited extent the results are not included in this report because their locations prevented direct comparisons with the other instruments.) Risø installed Kaijō Denki ultrasonic anemometers (sonics) and adjacent fast response thermocouples. From the measurements of sonic temperature (which was affected by the propane) and true temperature, the value of  $r$  was estimated by two different calculation methods, and these two sets of estimates were recorded on magnetic tape at 10Hz (although it appears that the actual response times of the methods - still uncertain - may be typically of order only 0.15s). Finally the results of these "fast" measurements of  $r$  were averaged to give "slow sonic" concentration measurements which were recorded, also at 1.25Hz, on the diskettes holding the catalytic measurements of  $r$ .

At the beginning of April Brunel had only the magnetic tapes (two sets of fast measurements) for 5 trials (EEC54-58) and diskettes (catalytic and slow sonic measurements) for 2 trials (EEC55, 57). (Unfortunately the data on these tapes were subsequently amended/revalidated by Risø, so analysis of the fast measurements could not begin until early June, when corrected tapes were received.) Near the end of May, complete records for EEC50-58 were received as were, in due course, data for other trials. For practical reasons (above all time in view of Brunel's tight schedule) and because the obstacle configurations were relatively simple and similar, Brunel placed most emphasis on trials EEC54-58 (but some analysis is available from the other trials).

*Figure 1* shows the obstacle configuration (one wall 2m high and 51.2m long) at the start of each of these trials but note that, as the experimental details in *Table 1* show, there were variations in obstacle porosity, source type, release duration and

whether/when the obstacle was removed. For these 5 trials, complete records of all 4 time series of measured values of  $r$ . were available at heights 1m, 2m and 4m on each of masts 3 and 4 (see *Figure 1*). (It must be noted that the catalytic type device was displaced 1.17m horizontally from the sonics but this does not affect the main points that will be made.)

Experiment Number	Release Rate (kg/s)	Obstacle Type	Release Duration (s)	Obstacle removed (s after start)	Wind speed (m/s)	Wind direction deviation	Source Type
EEC54	3.0	SOLID	300	NO	2.3	-35°	JET
EEC55	3.0	SOLID	360	185	2.6	-12°	JET
EEC56	3.0	50% POROUS	360	180	2.4	0°	JET
EEC57	2.0	SOLID	480	360	2.4	+10°	CYCLONE
EEC58	2.0	50% POROUS	480	360	2.6	+30°	CYCLONE

*Table 1* Experimental conditions for **EEC54-58**. Note that the release rates are those given by FOA's method, the wind speeds are 10 min averages at 10m height (extrapolated from measurements at 3.4m height) and the wind directions (10 min average at 3.4m height) give deviations from the "ideal" direction perpendicular to the obstacle.

*Figure 2* shows a typical comparison of the 4 different time series. There are several striking features of these and all similar comparisons. Taken as a pair, the two sets of 10Hz measurements exhibit higher peaks and much greater variability than the two sets of 1.25Hz measurements. However, there are differences between the two sets of fast data in that method 2 gives an even peakier signal than method 1 - higher maxima and lower minima. In fact the minima given by method 2 are substantially more negative than the noise minima (see the end of the record after  $t \approx 400$ s) and so there must be errors associated with this method. Whether these are significant will be discussed later. Although the 1.25Hz sonic measurements were obtained directly from the 10Hz data by averaging, it is clear that this operation results in substantial reductions in the perceived peak concentrations (by



up to 50%) and in the variability. There are clear correlations between the two sets of 1.25Hz measurements (see for example the strong peak in both just after  $t = 50\text{s}$ ); nevertheless the catalytic data is even less variable than the slow sonic data. In making these comments it has to be noted that the catalytic type devices were not designed, or expected, to measure concentration fluctuations accurately. It should also be recorded that the "fast" sonic data were validated against mixtures of known concentrations in laboratory trials and against the catalytic type devices in the field - but only by comparing mean concentrations; thus neither validation exercise involved concentration fluctuations. However, in a further comparison, the time series of  $r$ . was found to compare well with the time series of  $T$  from one of the Thorney Island experiments.

The next group of figures shows typical observed differences. *Figure 3* compares plots from EEC54 and EEC55 each taken at the same mast and height and using the same measurement method. That from EEC54 has a lower mean and, relatively, a greater variability than that from EEC55. Since the mast is 10m upwind of the wall, reference to *Table 1* shows that the only significant difference between the trials is the difference of about  $25^\circ$  in the mean wind direction, with the measurements in EEC54 being nearer the edge of the plume than in EEC55, and this is entirely consistent with the observed differences. *Figure 4* are plots from the same two experiments with the same method of measuring  $r$ . as in *Figure 3*, but at two different heights on the downwind mast 4. The wall remained in place throughout EEC54 but was taken down 185s after the start of EEC55, and the effects can clearly be seen. The wall has height 2m and lifts the plume; when the wall is removed the plume drops and the mean concentration level at 2m is reduced (from order 1.5% to order 0.5%). By contrast the mean level at 1m seems hardly to be changed, but there is a great increase in the variability which is not noticeable at 2m. The probable effects of wind direction deviation, already noted in *Figure 3*, are also apparent (but perhaps less markedly) when the EEC54 results are compared with the parts of the corresponding EEC55 results for times before the wall was removed. Finally *Figure 5* compares a jet release (EEC55) with a cyclone release (EEC57) for two of the measurement methods; the most striking difference is the expected lowering of the mean concentration level.

*Figure 6* shows a typical plot from a height of 4m for the fast sonic (method 1). Apart from the low level of concentration and very high relative variability, the degree of base line drift is a significant feature here, and entirely typical of plots from this height.

The differences between the measured concentrations for the different methods are further highlighted in *Table 2* and *Figure 7*. *Table 2* gives results of applying standard statistical techniques to the different datasets. The numerical values confirm visual impressions from earlier figures. The value of  $m$  is substantially lower for the catalytic type measurements than for the other measurement methods, except for the concentration at mast 3 in EEC55. For these two experiments at this height the values of  $m$  at mast 4 are always substantially higher than at mast 3, because the wall lifts the plume. In general the values of  $m$  at mast 4 are higher than those at mast 3 at 2m and 4m, but lower at 1m. The values of  $s$  at mast 4 are greater than those at mast 3, and this is true at all heights. Also the values of  $s$  are always in the order (increasing variability): 1.25Hz catalytic, 1.25Hz sonic, 10Hz sonic (method 1), 10Hz sonic (method 2). Calculations of skewness and kurtosis were also performed, but not included in this report. *Figure 7* shows scatter diagrams for one position (mast 3, height 2m) in EEC55 for the 6 pairwise comparisons possible. Each point shows the values of  $r$  at identical times as measured by the two methods indicated; for display purposes only a (relatively) small sample of such points are plotted. Ideally, i.e. all methods give identical results, all points should be on a straight line through the origin at  $45^\circ$  to each axis. That this is not the case except for the comparison between the two 10Hz methods is obvious. These visual impressions are confirmed by more formal statistical calculations, of which examples are shown in *Table 3*. Thus the difference between the two 10Hz methods - noted above in the comments on *Figure 2* - does not have statistical significance for the test of  $\beta = 1$ .

Method of measurement	Mast 3, height 2m			Mast 3, height 2m		
	m (%)	S (%)	s/m	m (%)	s (%)	s/m
10Hz sonic Method 1	0.23	0.32	1.39	0.61	0.43	0.70
10Hz sonic Method 2	0.23	0.36	1.57	0.61	0.44	0.72
1.25Hz sonic	0.24	0.21	0.88	0.62	0.34	0.55
1.25Hz catalytic	0.20	0.10	0.50	0.43	0.19	0.44

(a) EEC54

Method of measurement	Mast 3, height 2m			Mast 4, height 2m		
	M (%)	S (%)	s/m	m (%)	s (%)	s/m
10Hz sonic Method 1	0.39	0.44	1.13	0.79	0.55	0.70
10Hz sonic Method 2	0.39	0.51	1.31	0.79	0.57	0.72
1.25Hz sonic	0.41	0.22	0.54	0.83	0.43	0.52
1.25Hz catalytic	0.50	0.22	0.44	0.59	0.29	0.49

(b) EEC 55

*Table 2* Estimates of data mean (m) and standard deviation (s). Since the experiments are not statistically stationary, m and s are not estimates of  $\mu$  and  $\sigma^2$  (defined in §2.1), but serve to quantify the overall level and the variability of the data, and also to discriminate between the different methods of measurement. The values of s/m are, as it happens, not untypical of estimates of the intensity  $\sigma/\mu$  obtained for other atmospheric dispersion data.

Comparison	r	99% CI for $\rho$	$\alpha$	$\beta$	Test result
10Hz sonic 1 vs. 10Hz sonic 2	0.92	[0.89,0.95]	0.00	1.01	ACCEPT
1.25Hz sonic vs. 1.25Hz catalytic	0.72	[0.63,0.81]	-0.13	1.20	REJECT

**Table 3** Some examples of statistical results for the pairwise comparisons shown in *Figure 7*.

r is the sample correlation coefficient and is used to obtain the confidence interval (CI) for the population correlation coefficient  $\rho$  - note that  $\rho$  would equal 1 for two methods giving ideal (i.e. identical) measurements of r. The coefficients  $\alpha$ ,  $\beta$  are those in the line of regression  $y = \alpha + \beta x$ , where x is the result of the first method named. The last column shows the results of a standard significance test with the null hypothesis  $H_0$  being that  $\beta$  has the value 1.

One of the most common measures used to assess the harm caused by a dangerous (usually toxic) gas is the dosage  $D(t)$ , where

$$D(t) = \int_0^t r(s) ds. \quad (8)$$

Despite the significant differences between the four methods of measuring  $r$ , the calculated dosages were much closer than might have been expected. In particular, as the typical *Figure 8* shows, the three methods employing the sonics gave practically indistinguishable results. Since the 1.25Hz sonic data were obtained by averaging the fast sonic data, this equality could of course have been anticipated. What is surprising is that  $D$  obtained from the catalytic data is no more than 20% less than the values obtained from the sonic data - much more might have been expected from superficial glances at *Figures 2* and *7*. *Figure 9* compares the dosages from a jet release (*Figure 9(a)* - EEC56) with those from a cyclone release (*9(b)* - EEC57). Reference to *Table 1* shows that the walls in these experiments differed (EEC56 - 50% porosity; EEC57 - solid wall) and that EEC57 was a longer

trial. Nevertheless the outstanding difference, viz. that the dosages in EEC57 are substantially lower than the dosages at the corresponding positions in EEC56, is undoubtedly due to the difference between the source types. The dosages in *Figure 9(b)* are, of course, still rising at the highest time shown on the figure; due to the lack of downwind momentum at release the cloud takes longer - much longer - to pass a given sensor than for a jet release. It will also be noted that the dosages at both masts at a height of 4m are at least an order of magnitude less than at a height of 1m. There is now some evidence that a better measure of harm than  $D(t)$  in (8) may be  $D_n(t)$ , where

$$D_n(t) = \int_0^t r^n(s) ds, \quad (9)$$

and the value of  $n$  depends on the particular gas; values of  $n$  in the range 2.5 to 3 have been proposed for gases like chlorine and ammonia. Although not included in this report, graphs of  $D_n(t)$  for  $n=2, 3$  for the TuV/Ris $\phi$  data are available.

It has already been noted that the TuV/Ris $\phi$  trials are not statistically stationary releases, and therefore that statistical properties like  $\mu$  and  $\sigma^2$  cannot be estimated from the record of one release on a rigorous statistical basis. (See the caption to *Table 2*.) Nevertheless there is evidence from the time series (see *Figures 2 to 6*) that the central portions of records are, to at least a rough approximation, what might be anticipated from a statistically stationary release. On this basis, very many histograms were plotted and some are shown in *Figures 10 and 11*. *Figure 10* compares, for one position upwind of the wall in EEC55, the histograms obtained for the four different methods of measurement. As expected, those obtained for the two fast some methods are very comparable. The averaging involved in obtaining the slow (1.25Hz) sonic data results in significant lowering of the proportion of time that a very low concentration was recorded, and also a reduction in the proportion of times (relatively) very high concentrations were observed. The histogram obtained from the catalytic measurements is different again. All these features are consistent with points noted in the discussion of earlier figures. Each of the histograms records a fairly substantial proportion of negative concentrations; although negative concentrations are impossible, the data also includes inherent noise and - in the case of method 2 for the 10Hz sonic data - contributions that are

erroneously calculated - see comments on *Figure 2*. For histograms of adequate length of true statistically stationary releases, it would be possible and advisable to remove noise from the signals using methods such as those described by Mole (1989a, 1989b, 1990) - see papers listed in §1.4. Another feature of histograms for atmospheric dispersion releases is that, due to practical limitations on pixel size, they often do not show the highest concentrations recorded. This is evident from a visual comparison of the fast sonic data as recorded in time series form in *Figure 2* with the same data in histogram form in *Figure 10*. One might note also - but with due caution for the reasons already emphasised - that the histograms for the two 10Hz sonic data have the characteristic "exponential" shape exemplified in other atmospheric dispersion datasets. *Figure 11* shows histograms from the mast downwind of the wall at two heights for EEC56 with (on the left) those obtained from the data before the wall was removed and (on the right) those obtained after it was removed. One notices primarily the change at height 2m in the overall mean level; this was also noted (in similar circumstances) for EEC55 - see the comments above on *Figure 4*.

The final diagrams in this report on the TuV/Risø data also illustrate different facets of the changes in behaviour of the concentration measurements due to the removal of the wall in EEC55 at mast 4 (downwind) at height 1m. *Figure 12* shows plots of  $C(t)$  versus  $C(t+20s)$  for three time regimes: (a)  $(t+20s) < t_o$ ; (b)  $t < t_o, (t+20s) > t_o$ ; (c)  $t > t_o$ , where  $t = t_o$  is the time at which the wall was removed. The differences between these three scatter-plots are manifest and, in particular, the greatly increased variability after the removal of the wall has been noted for this height in *Figure 4*. Similar behaviour was noted for other "lag" times of the order of 20s. Finally *Figure 13* presents an empirical algorithm which shows that  $t_o$  can be detected to within 1s. Note that *Figure 13(c)* is an enlargement of the relevant portion of *Figure 13(b)*. Time has not permitted further investigation of the points illustrated by these final two figures. It would clearly be desirable to establish proper non-dimensional forms for both figure calculations - and there is no doubt that this would be possible - and to provide a theoretical basis for the algorithm in *Figure 13*.

### 3.3 Data from TNO

TNO was one of the three institutes which conducted wind tunnel experiments. For various reasons, referred to earlier and mainly to do with data recording and transmission, Brunel was not able to give as much attention to the TNO data as, ideally, would have been the case.

The experiments were conducted in the Pollution Industrial Aerodynamics (PIA) wind tunnel of TNO. The gas released in all cases was  $SF_6$ , and its concentration was measured with an aspirated hot wire probe whose frequency response was estimated at 70Hz. Data were recorded at 60Hz. Details of the tunnel and the instrumentation are contained in the companion report by TNO; in preparing this account, particular use has been made of a report by H. van Oort and P J.H. Builtjes entitled *Instantaneous and Continuous Release Tests for Intercomparison of Experimental Equipment*, **MT-TNO Ref. No. 90-346**, dated October 1990.

As noted earlier, the TNO data were received on discs in a readable form at the end of April 1990. There were three different dataset groups, all intended for intercomparison with data taken by UH and WSL under experimental conditions (wind tunnel turbulence, source type and strength, ...) designed to be identical (as nearly as possible).

The first group of experiments were a model of Thorney Island Trial No.17. Details of these instantaneous releases - seven in all - are given in *Tables 4* and *5*, and *Figure 14* shows the time series obtained at Brunel by Mr. Goodall. The same probe was used for each release, but there is evidence for releases 02 - 05 of substantial base-line drift. Although this drift accelerates with time and may, therefore, not be significant during the passage of the central portion of the gas cloud, its ultimate magnitude is somewhat disturbing.

<b>EXPERIMENT</b>	$V_o$ ( $m^3$ )	$\frac{\rho - \rho_o}{\rho_o}$	$L_{ci}$ (m)	$T_{ci}$ (s)
<b>Thorney Island Trial No.17</b>	1700	3.2	11.9	0.6
<b>TNO Instantaneous Releases</b>	0.0014	4.12	0.112	0.053

*Table 4* Comparison of experimental conditions. ( $V_o$  is volume of gas released,  $\rho$  is initial gas density,  $\rho_o$  is air density and  $L_{ci}$ ,  $T_{ci}$  are the characteristic length and time scales - see UH progress report by Professor Dr. M. Schatzmann, dated June 1988.)

TNO experiment (File No.)	$\frac{x}{L_{ci}}$	$\frac{y}{L_{ci}}$	$\frac{z}{L_{ci}}$
INST 01	1.87	1.68	0.034
INST 02	3.12	2.79	0.034
INST 03	4.37	3.92	0.034
INST 04	5.61	5.04	0.034
INST 05	5.91	-0.33	0.034
INST 06	8.88	-0.48	0.034
INST 07	11.84	-0.64	0.034

*Table 5* Location of the probe in each of the seven releases, with x downwind, y lateral, z vertical. (Figures taken from October 1990 TNO report - there are some differences from figures on the disc.)

The second group of experiments were six continuous releases ( $\dot{V}_o =$  release rate =  $1.744 \times 10^{-4} m^3/s$ ;  $L_{cc} = 0.015m$ ;  $T_{cc} = 0.019s$  - where  $L_{cc}$ ,  $T_{cc}$  are the characteristic length and time scales for continuous releases defined by Professor Schatzmann.) In CONT01 - 04, conditions were identical, but there were differences in the four probe positions (as shown in *Table 6*). In the remaining two trials the wind speed was halved (CONT05) and doubled (CONT06) with respect to the first four trials. The twenty-four time series are shown in *Figure 15*. Several of these are at identical locations for repeat releases. For example, CONT0101,



CONT	0101	0102	0103	0104
$x/L_{cc}$	42.7	85.5	128.2	171.0
CONT	0201	0202	0203	0204
$x/L_{cc}$	42.7	85.5	128.2	171.0
CONT	0301	0302	0303	0304
$x/L_{cc}$	42.7	213.7	256.4	299.5
CONT	0401	0402	0403	0404
$x/L_{cc}$	42.7	213.7	256.4	342.3
CONT	0501	0502	0503	0504
$x/L_{cc}$	42.7	85.5	128.2	171.0
CONT	0601	0602	0603	0604
$x/L_{cc}$	42.7	85.5	128.2	171.0

*Table 6* Probe positions for each of the six continuous releases. (In each case  $y = z = 0$ ).

CONT0201, CONT0301 are all at  $x/L_{cc} = 42.7$  with the same wind speed, yet the means are clearly different. In principle, and provided the wind tunnel turbulence and source conditions are the same, the long-term time means should be the same for these cases. The fact that they are not could be due to an inadequate length of the data records or, more seriously, to changes in instrument behaviour (e.g. baseline setting, zero drift). Apart from the evidence already obtained from the instantaneous releases of somewhat unsatisfactory instrument behaviour, the traces in *Figure 15* provide further causes for concern. For example, the mean concentration in CONT0402 is below that in CONT0403, yet the latter is taken further downwind. Moreover several of the time series appear to be skewed with a tail towards the lower concentrations (e.g. CONT0101, CONT0201, ...); this behaviour is very atypical of results from other experimenters - e.g. *Figures 10* and *11* above.

The third group of data received from TNO consists of 53 runs, all conducted under conditions modelling the full-scale trial EEC57 conducted by TuV/Risø - see §3.2 and, especially, *Table 2* for details of the experiment. Each run consisted of the

record from one instrument that was moved from position to position during the series. From the point of view of Brunei's data analysis, it was unfortunate that none of the measurement sites chosen by TNO corresponded with one of the two sites at which sonic measurements and catalytic-type measurements were taken. Thus the more detailed intercomparison that mainly motivated the wind-tunnel trials (at UH and WSL, as well as TNO) was not possible during the present programme. For that reason only a few records are shown in this report. There were 9 triplets of runs called TUV0xxx; each triplet consists of a run without a wall, a run with a wall and a run where the wall was removed after 30s ( $\approx 2143T_{cc}$ ). (In the "real" EEC57 the wall was removed after 360s of a run lasting 480s.) *Figure 16* shows the sensor positions in EEC57 (received from TNO via UH) and also those modelled in the TNO experiments. *Figure 17* shows the results from TUV0301 – 0303 taken at position 35, just downwind of the wall. One notes that, unlike the sonic data from the real EEC57 (although from a different position) shown in *Figure 5*, there is hardly any proportion of the record for which the concentrations were very low. There were also 6 quintuplets of runs labelled TUV1xxx; each quintuplet consisted of a run with no wall, two runs with walls aligned at  $+15^\circ$  and  $-15^\circ$  to the "ideal" direction (used in TUV0xxx) and two runs with the walls removed after 30s. (The set TUV11xx is in fact a sextuplet because the no-wall case was measured twice.) *Figure 18* shows the results from TUV1201 - TUV1205, also taken at position 35 (like the data in *Figure 17*). It is believed that fence alignment can have substantial effects on the concentration; this cannot be asserted from the results shown since the inherent variability is too large. But further analysis is planned. It is also important to note that baseline drift needs further consideration in view of earlier comments; there is evidence of this from the record TUV1203 for example.

### **3.4 Data from WSL**

As with the other datasets considered in this report and analysed at Brunel, reference should be made to source reports for full details of experimental conditions. In writing the present text, reference was made in particular to a confidential contract report by Dr. DJ. Hall and his colleagues Mr. GA. Marsland and Mr. MA. Emmott entitled *CEC-MTH Wind Tunnel Intercomparison of Heavy Gas*

*Dispersion*, **CR 3256 (PA)** and dated April 1990. Further information, particularly of the experimental apparatus and procedures, is given in a report with the same authors plus Mr. RA. Waters and Mr. SL. Upton entitled *Repeat Variability in Instantaneously Released Heavy Gas Clouds - Some Wind Tunnel Model Experiments*, **LR804(PA)** and dated January 1991. (The latter report was not available in its final form during the preparation of this Brunei report.)

The experiments were all performed in WSL's No.1 wind tunnel, which is of the open circuit type with a working section of 22m (length)  $\times$  4.3m (width)  $\times$  1.5m (height). *Figure 19* shows the layout in all the trials. The gas source, a 1/100 scale model of that used at Thorney Island, was a cylindrical tent, 0.13m high and 0.14m in diameter. As in the Thorney Island trials, gas was released almost instantaneously by collapsing the tent, using a well-proven design. The collapse time was about 0.2s.

Experiments were performed for 6 different Richardson Numbers Ri, where

$$Ri = \frac{g\Delta\rho H}{\rho_o U^2}, \quad (10)$$

and the symbols have the following (standard) meanings: g = acceleration due to gravity; H = gas tent height; U = mean wind speed at height H (measured far upwind of the tent);  $\rho_o$  = density of ambient air;  $\Delta\rho = (\rho_{gas} - \rho_o)$  where  $\rho_{gas}$  = density of source gas. *Table 7* gives further experimental details. For Ri = 5, 10 the gas used was BCF (with chemical formula  $CBrClF_2$ ), for Ri = 1, 2 the source gas was a 50% mixture of BCF and air, and for Ri = 0.5 the gas used was argon (with a small amount of methane tracer). Concentration measurements for releases involving BCF were made with catharometers (response times from about 0.01s at concentrations of 50% to about 0.03s at 100%) and those at Ri = 0.5, 0 were made with FIDs (flame ionisation detectors) of the Cambustion design (response times of order 0.01s).

WSL have, in recent years, undertaken several series of experimental programmes using the same layout, techniques and values of Ri. Those in the MTH Programme were jointly funded by HSE and included fences (both solid and crenellated, and of

various heights) at 1.0m downwind of the gas tent. In a slightly earlier series, wholly funded by HSE, there were no fences. All the tests involved multiple repetitions (50 or 100). In April 1990, Brunel had received the 'no fence' data (except for  $Ri = 0.5$ ) from HSE, but the 'fence' and other data tapes did not arrive until early June 1990 and then needed substantial reformatting. The total quantity

Ri	U ( $ms^{-1}$ )	$\frac{\Delta\rho}{\rho_o}$	n	H/U (s)	Tci (s)
10	0.78	4.75	50	0.17	0.052
5	1.10	4.75	50	0.12	0.052
2	1.20	2.37	100	0.11	0.074
1	1.74	2.37	100	0.07	0.074
0.5	0.98	0.38	100	0.13	0.184
0	0.98	0	100	0.13	-

*Table 7* Experimental details for WSL's no fence data. In addition to symbols defined in the text, n is the number of repeat runs and  $T_{ci}$  is the time scale for instantaneous releases of heavy gases defined by Professor Schatzmann. ( $T_{ci} = V_0^{1/6} (g')^{1/2}$  where  $g' = g\Delta\rho / \rho_0$  and  $V_0 \approx 2 \times 10^{-3} m^3$  is the volume of the source.)

of WSL data is about 0.2gb, and resources and time did not allow all the data to be analysed in the detail that is undoubtedly merited. Following the philosophy behind Brunel's contribution that was discussed in Chapter One, attention was primarily given to the 'no fence' data that were available at the beginning of the period when analysis was undertaken. Since that has terminated, further analysis has been performed and will continue (partly as a contribution to work in the FLADIS project). Results will be reported in due course and as appropriate.

In this report, the results shown and discussed are typical, not comprehensive, and have been selected to be, where possible, complementary to analyses presented by

HSE, and by WSL itself. *Figure 20* illustrates the typical nature of a raw signal obtained in these trials. Data were collected by sampling at 100Hz, beginning prior to the tent collapse to provide a reference level for zero concentration. This procedure also indicated noise levels which, consistent with *Figure 20*, were of the order of 0.05 - 0.15%. This signal shows that the first indication of the gas was a very sharp peak, representing the leading edge arrival, followed by a drop and then a more gradual rise to a second and higher peak, representing the bulk of the gravity current. As many further traces of the same sort show (see WSL Report LR 804 (PA) referred to above) this bimodal feature was present nearly always for  $Ri = 10$  and sometimes for  $Ri = 5$ . The second peak only was evident at this near ground-level station for  $Ri = 2$  (and occasionally for  $Ri = 1$ ). Naturally no such effects were observed for  $Ri = 0$ . After the first arrival and the maximum concentration signal, there is a gradual decay with obvious random variations.

The large numbers of repeats enabled estimates of some statistical properties to be made by standard methods. (It will be noted that this is a very valuable and unusual feature of the WSL experiments, and indeed was one of the principal motivations for conducting them. Instantaneous, or, more generally, non-stationary releases, are the norm in real-life situations involving the accidental release of dangerous gases. Although stationary (i.e. steady continuous) releases are much more popular in experiments, presumably because statistical properties can then be estimated by time averages, great caution is needed in applying the results to realistic hazard assessment scenarios. There is consequently a need for further experiments like those at WSL, costly and time-consuming though they may be.) The next group of Figures show some typical results. In the discussion  $m = m(t)$  and  $s = s(t)$  will denote the estimates of  $\mu(t)$  and  $\sigma(t)$  respectively, defined in (4) and (5) in Chapter Two. *Figures 21* and *22* are from the lower station at 0.7m downwind, and *Figures 23* and *24* are from the lower station at 2.0m downwind. Among the points of interest are:

(a) In *Figures 21* and *22*, there is a clear difference in behaviour between  $Ri = 10, 5, 2$  on the one hand, and  $Ri = 1, 0$  on the other. The predominant feature of the graphs of  $m(t)$  for the former is the large maximum soon after arrival that has persisted from the separate realizations throughout the averaging process. It seems

remarkable, moreover, that for  $Ri = 10$  the bimodal structure noted in *Figure 20* for one single run has also persisted.

(b) The maximum values of  $m$  for  $Ri = 10, 5, 2$  in *Figure 21* are of the order 10%, whereas for  $Ri = 1, 0$  they are of order 5%. Furthermore, the graph for  $Ri = 1$  is qualitatively similar to that for the neutrally buoyant case  $Ri = 0$ . This suggests that mixing has already caused the  $Ri = 1$  gas cloud to behave essentially as a passive tracer with the gas spread out much more in the vertical direction than for the higher values of  $Ri$  at this distance downwind. (Partial confirmation of this is provided by *Figure 25* which shows how much smaller  $m$  is for  $Ri = 10$  than for  $Ri = 0$  at the higher station at 0.7m downwind.)

(c) By contrast *Figure 23* shows that the graphs of  $m(t)$  are all qualitatively similar at 2.0m downwind, except for the much sharper nature of that for  $Ri = 0$ . The likely explanation is that, at this distance downwind, heavy gas effects have essentially disappeared (even for  $Ri = 10$ ) except for a legacy - almost describable as inertia, which is that there is a measurable quantity of slow-moving gas near the ground which therefore causes 'tails' due to the relatively long time taken for such gas to reach, and pass, the sensor.

(d) In *Figure 22*, the maxima in the graphs of  $s(t)$  are sharp and occur almost simultaneously with the maxima in  $m(t)$ . Two factors would lead to increased variability at (or near) such times. One is the intense turbulence generated by heavy gas effects and the other is differences between separate realizations in the arrival times at the sensor; no attempt has been made yet to distinguish the magnitudes of these contributions.

(e) The most remarkable feature of *Figure 24* is, perhaps, the low values of  $s(t)$ , very rarely exceeding 1%. But, although the maxima for  $Ri > 0$  are very weak they clearly occur after the corresponding peaks in the graphs of  $m(t)$ . The obvious, and most likely, explanation is that given in (c) above - namely the slow-moving gas in the tails of the cloud.

(f) Apart from the importance of  $\sigma$ , and therefore its estimate  $s$ , in its own right in statistical models of heavy gas (and neutrally buoyant gas) dispersion, it can also be used to measure the uncertainty in the estimates of  $\mu$  shown in *Figures 21* and *23* since the standard deviation of such estimates is  $(\sigma/\sqrt{n}) \approx (s/\sqrt{n})$ . Reference to *Figures 22* and *24* (and *Table 7* for values of  $n$ ) shows that  $(s/\sqrt{n})$  is of order 4 -

9% of the maximum of  $m$  in *Figure 21*, and of order 3 - 4% of the maximum of  $m$  in *Figure 23*. (As is well known, the appearance of  $\sqrt{n}$  (rather than, say,  $n$ ) means that substantial reduction in this uncertainty is very costly to achieve.)

(g) *Figure 26* shows the estimates of  $s$  for the higher station at 0.7m downwind for  $Ri = 10$  and  $Ri = 0$ , and should be considered with *Figure 25*. Unlike the situation at the lower station the  $s$  values for  $Ri = 0$  are higher than those for  $Ri = 10$  both because the neutrally buoyant cloud is spread out more vertically and, presumably, because the sensor position is close to the top of the cloud for  $Ri = 0$  but (usually) far above it for  $Ri = 10$ .

There are two somewhat more general comments that seem important at this point. First, because the concept of using scientifically well-based statistical models for the atmospheric dispersion of gases is relatively novel, especially for practical problems, there is at present an inadequate body of knowledge about the structure of such models and, more particularly, about the forms of the pdfs. (Statistical experience from other fields usually relates to random variables which, unlike  $r$ , are not (or need not be regarded as) inherently positive.) In these circumstances, more theoretical work needs to be done - see (f) above - to assist in the design of experiments to ensure that, as far as possible, robust estimates of statistical properties can be obtained from the results of the experiments. Such work is being undertaken by Mr. Goodall using the WSL data, and results will be reported soon. The second point to be made is illustrated by the contrast noted in (a) and (b) above between the  $Ri = 10, 5, 2$  data on the one hand and the  $Ri = 1, 0$  data on the other. At 0.7m downwind in the WSL experiments the  $Ri = 1$  gas cloud was already behaving essentially as if neutrally buoyant. By 2.0m downwind - see (c) above - all the clouds appeared to be evolving as if neutrally buoyant except for the pronounced tails. The question of how to model satisfactorily the transition from heavy gas behaviour to passive tracer behaviour is an old one in this field, and poses great difficulties also for the deviser of statistical models. The authors of this report wish to note that this is an area of great importance. It is fortunate that it has a high priority in the FLADIS project.

There has been much academic interest in the behaviour of the concentration

intensity  $\sigma/\mu$ , particularly in regions (of space or time) where both become small. Some protagonists argue that  $\sigma/\mu$  approaches 0, and others that it approaches a positive constant. While, to the writers of this report, the value of  $\sigma/\mu$  seems much less important and interesting than the separate behaviours of  $\mu$  and  $\sigma$ , it was easy and natural to estimate  $\sigma/\mu$  from the WSL data by  $s/m$ , and it can be reported that in no case did it appear to approach zero. *Figure 27* gives two typical examples, chosen almost at random. More pertinent to the development of useful statistical models is the investigation of much more widely applicable relationships between  $\sigma$  and  $\mu$  such as those considered at length by Dr. Davies in the HSE report on the MTH project that corresponds to this one. Another relationship of the same genre, well-validated for stationary releases in the laboratory, is (7) of Chapter Two. Whether this is useful in non-stationary situations is not known, but the WSL data are being used to investigate this. *Figure 28* is one example of a plot of  $s^2$  against  $m$  that appears to show the parabolic behaviour of (7) in the region where  $0 \leq m \leq 5$ , but not for greater values. Reference to *Figure 21* shows that these higher values of the mean are associated with the peak as the cloud first arrives at the sensor. Although some of the theoretical support for (7) applies to this region, some of it does not. (In particular, the self-similar structure - if any - appropriate to the present trials is different in type from that associated with steady, non-buoyant, releases in laboratory jets etc.). All that can be said at this stage is that investigations are proceeding.

Histograms for all the data have been obtained but, except for the two typical examples shown in *Figure 29*, are not included in this report. For one thing, analysis which has a similar purpose in many respects is contained in great detail in WSL's Report LR 804 (PA) and for another, these plots are less pertinent than estimates of the pdf (which require the same input). The two diagrams in *Figure 29* are both for the lower station at 0.7m downwind and each shows histograms at  $\tau = Ut/H = 2.5, 5, 10, 15, \dots$ , where  $t$  is the time since release. In both cases ( $Ri = 10$  and  $Ri = 0$ ) the histogram for  $\tau = 2.5$  represents 'pure' noise and confirms that this is distributed symmetrically about zero. Subsequent histograms ( $\tau > 5$  for  $Ri = 0$ ) show the effect of the gas and confirm that the noise is indeed small (as



noted above). The contrast between the two diagrams (e.g. for  $\tau = 10$ ) represents the differences already noted in discussing *Figures 21* and *22*; particularly striking is the much longer time taken for the  $Ri = 10$  cloud to pass the sensor. Note that the final histogram in each diagram shows that there is still substantial gas upwind of the sensor since these histograms are not the same as those at  $\tau = 2.5$ . Estimates of the pdf for the data are being made now under Mr. Goodall's direction at Brunel as part of the more basic investigation referred to earlier.

Finally *Figure 30* shows some typical dosage plots, where dosage  $D(t)$  is defined in (8). The order at the lower station at 0.7m is as expected from the earlier discussion of *Figures 21* and *22*, but those on the other graphs is not so easy to explain except that it appears likely that asymptotic values have not yet been reached.

## **CHAPTER FOUR: CONCLUDING REMARKS**

### **4.1 Lessons and recommendations**

It will be clear that the quantity of data generated in the experimental programmes in Project BA was much greater than Brunel had anticipated at the outset of the contract, and much more than it could analyse within the time and resources made available. As indicated in several places in the text, these datasets are now being, and will continue to be, used as part of the basic research programme of the authors.

To some extent, Professor Chatwin should have realized rather earlier than he did that this problem of sheer data quantity would arise; had he done so, the analysis exercise at Brunel might have been better planned. Nevertheless, there were other connected problems outside his, and Brunel's, control that seem worth commenting on here since they have implications for future research, including FLADIS. Present data acquisition and storage systems are such that in experiments there is now a real danger that far more data are transmitted to analysts and modellers than can ever be properly used - certainly with the staff resources likely to be available. There is an argument that as much good quality data as possible should nevertheless be collected since it serves as a valuable databank for future workers; there is of course some point to this, but one is somewhat sceptical about whether the whole databank, or even a substantial portion, is ever used in such cases. But there is a counter-argument, namely that in projects like BA and FLADIS the limited time-scale requires any one data set to be such that its general contents can rather easily (and quickly) become familiar to the analysts, for only then can they operate with the control and discrimination that is so highly desirable in scientific research, especially research involving many collaborators.

In summary, Brunel underestimated its task; so perhaps did some of our partners in Project BA since there were unfortunate - but entirely explicable - problems with the delivery on time, and in an appropriate format, of some tapes. There is a clear lesson for all future collaborative projects in this area - namely that, with present data acquisition capacities, far more attention needs to be paid to experimental

design *before* any resources are irrevocably committed, and that experimental design should include the time and staff available to the analysts. Moreover close liaison (and prior agreement) is needed to ensure that different institutes' computing systems are compatible, and that there is agreement beforehand on the goals of the analysis.

## **4.2 Acknowledgements**

We wish to thank Peter Burge and Stephen Decent for their skill and enthusiasm in producing the tables and figures discussed in this report, and Molly Demmar for showing her customary expertise in producing a readable version of our text. Philip Chatwin wishes to thank his co-author Gerald Goodall both for sharing the direction of this analysis, and for his constant and continuing interest in this work. We have appreciated the support of CEC, and the interest and professional skills of Peter Storey and our Project BA partners. Above all, it would be remiss not to place on record our great gratitude to the project coordinator Peter Builtjes both for his cheerful administration, and for his invaluable scientific input.

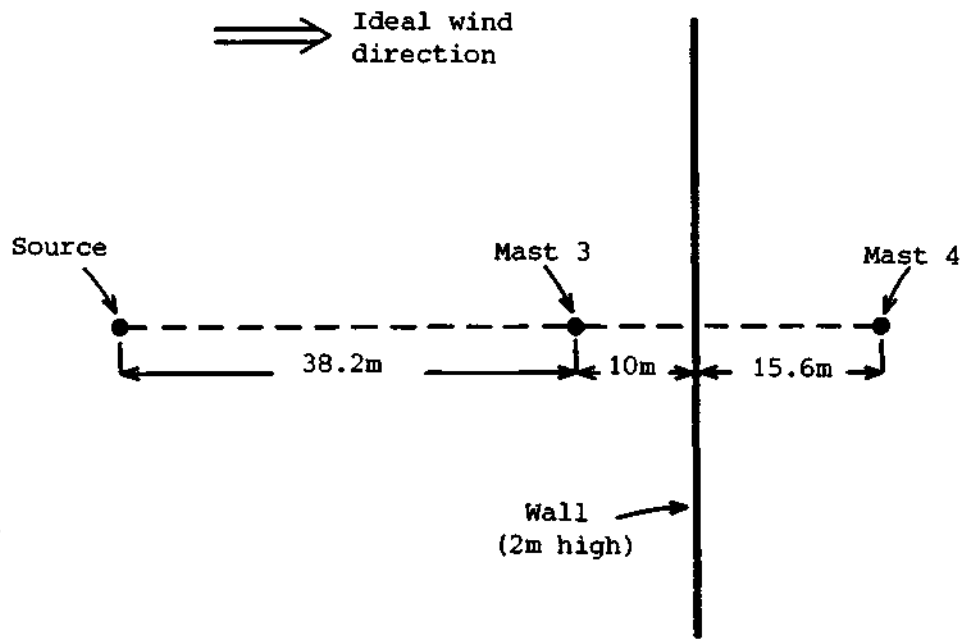
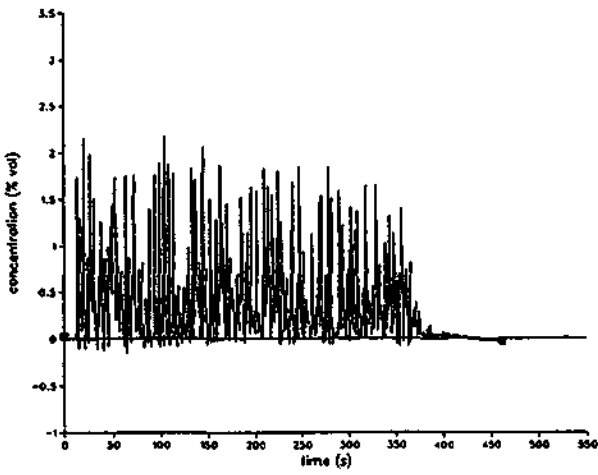
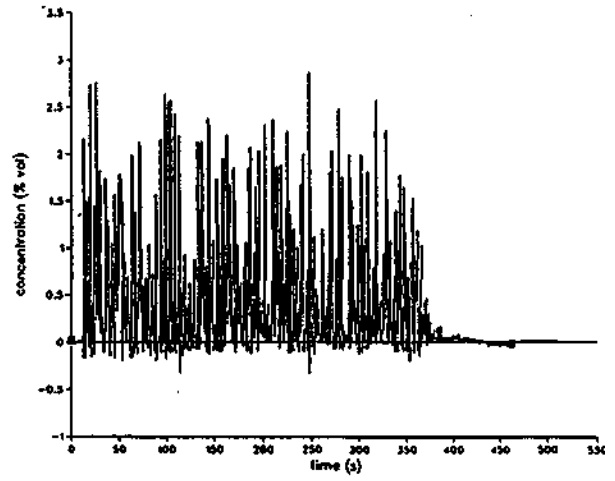


Figure 1 Experimental layout for EEC 54-58.

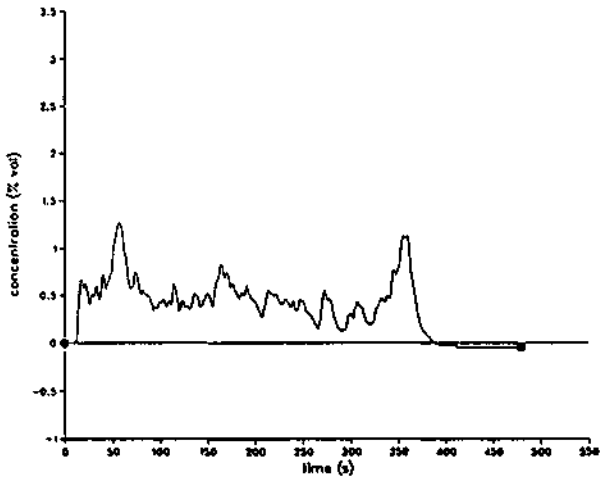
EEC55 mast3 height 2m, 10Hz sonic, calc method 1



EEC55 mast3 height 2m, 10Hz sonic, calc method 2



EEC55 mast3 height 2m, 1.25Hz catalytic



EEC55 mast3 height 2m, 1.25Hz sonic

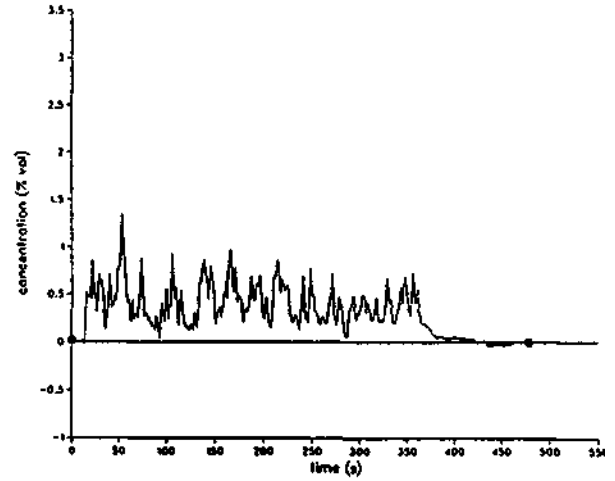
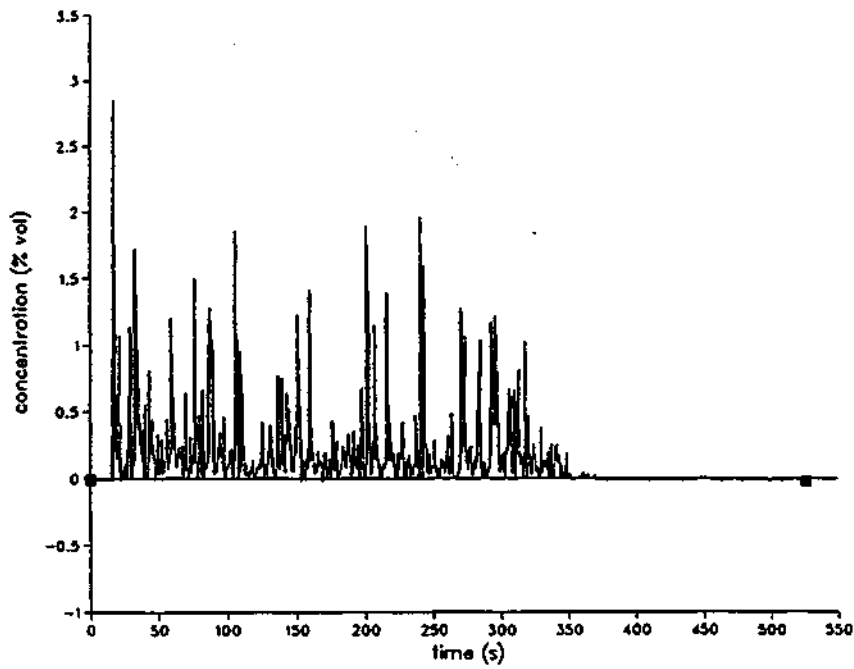


Figure 2 A typical comparison of time series obtained by the four different methods.

EEC54 mast3 height 2m,10Hz sonic, calc method 1



EEC55 mast3 height 2m,10Hz sonic, calc method 1

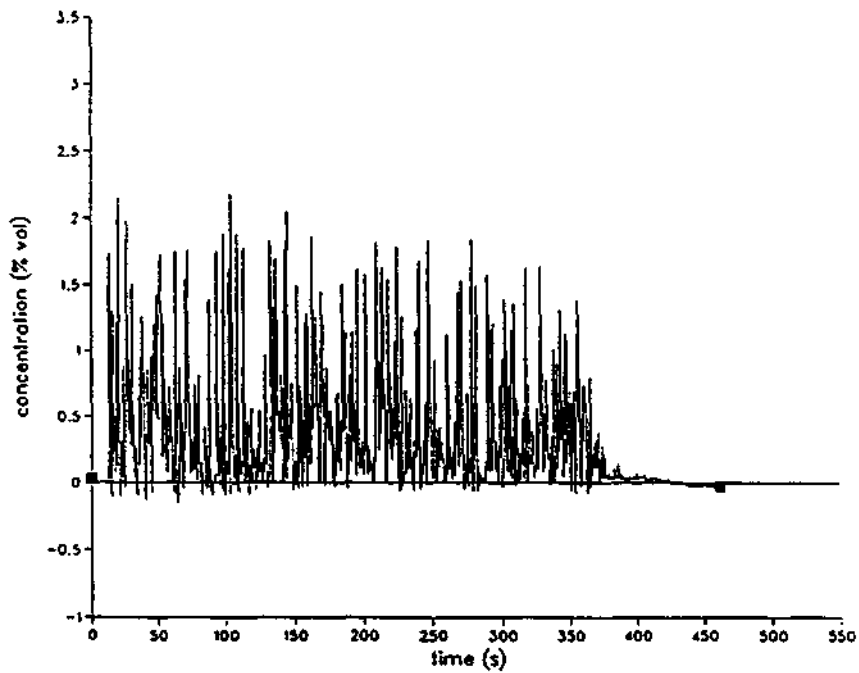
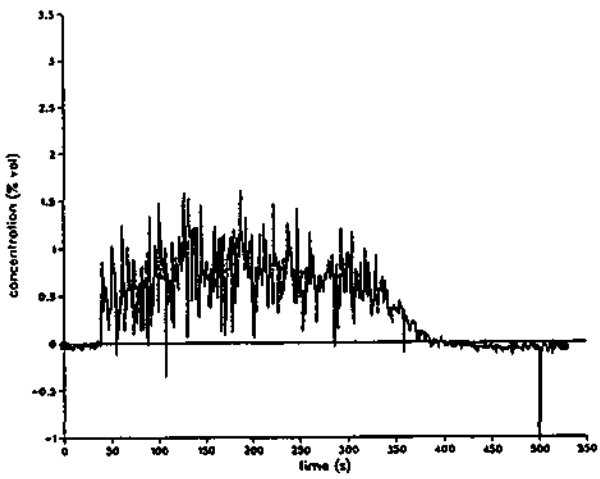
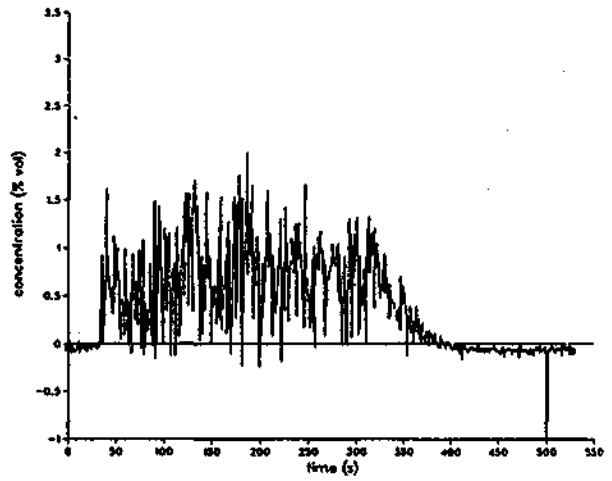


Figure 3 Comparison between different experiments (see Table 1 for details) with same measurement method at same station.

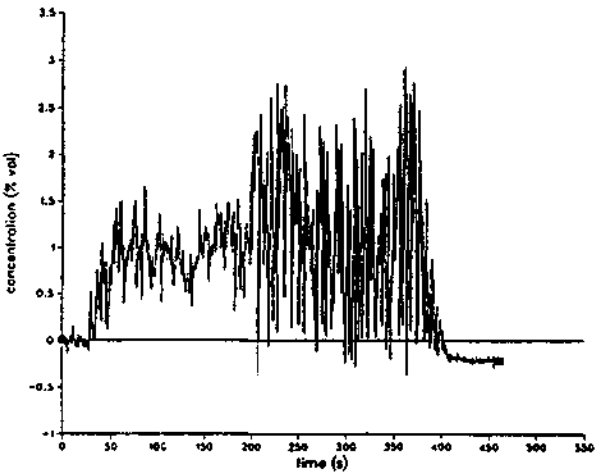
EEC54 mast4 height 1m,10Hz sonic, calc method 1



EEC54 mast4 height 2m,10Hz sonic, calc method 1



EEC55 mast4 height 1m,10Hz sonic, calc method 1



EEC55 mast4 height 2m,10Hz sonic, calc method 1

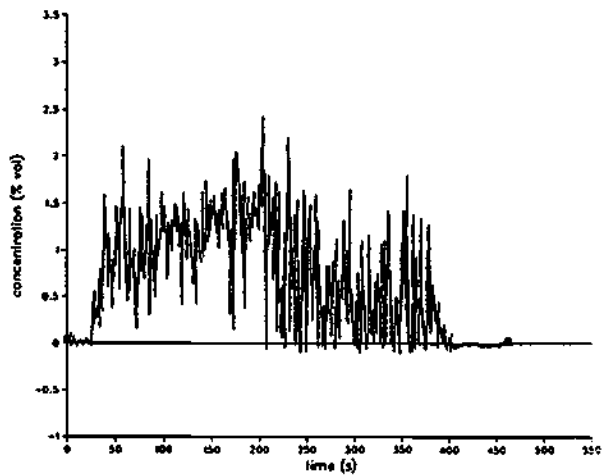
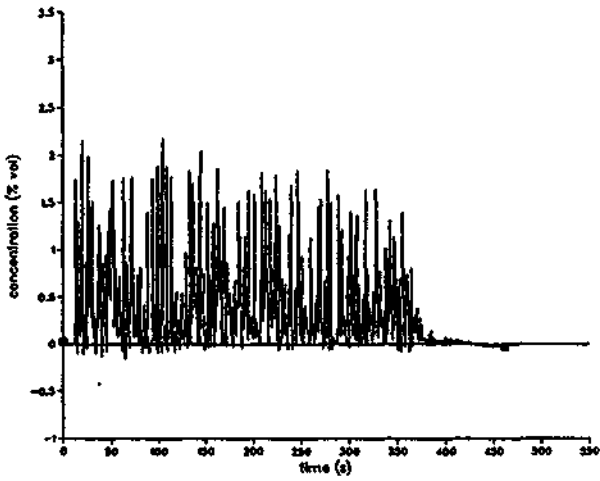
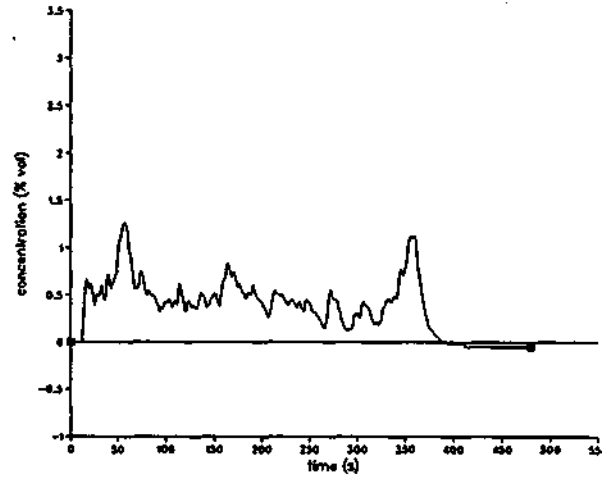


Figure 4 Effect of wall on time series at Mast 4 (see Figure 1). In EEC 54, the wall remained in place throughout; in EEC 55, it was taken down after 185s.

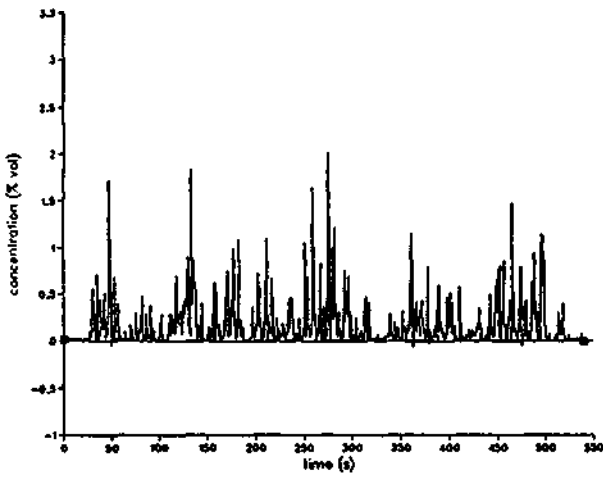
EECS5 mast3 height 2m, 10Hz sonic, calc method 1



EECS5 mast3 height 2m, 1.25Hz catalytic



EECS7 mast3 height 2m, 10Hz sonic, calc method 1



EECS7 mast 3 height 2m, catalytic

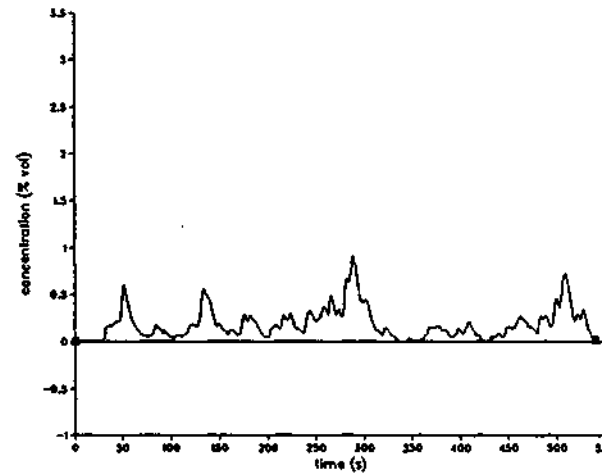


Figure 5 Comparison, for two of the measurement methods, of a jet release (EEC 55) with a cyclone release (EEC 57).



EEC56 mast4 height 4m,10Hz sonic, calc method 1

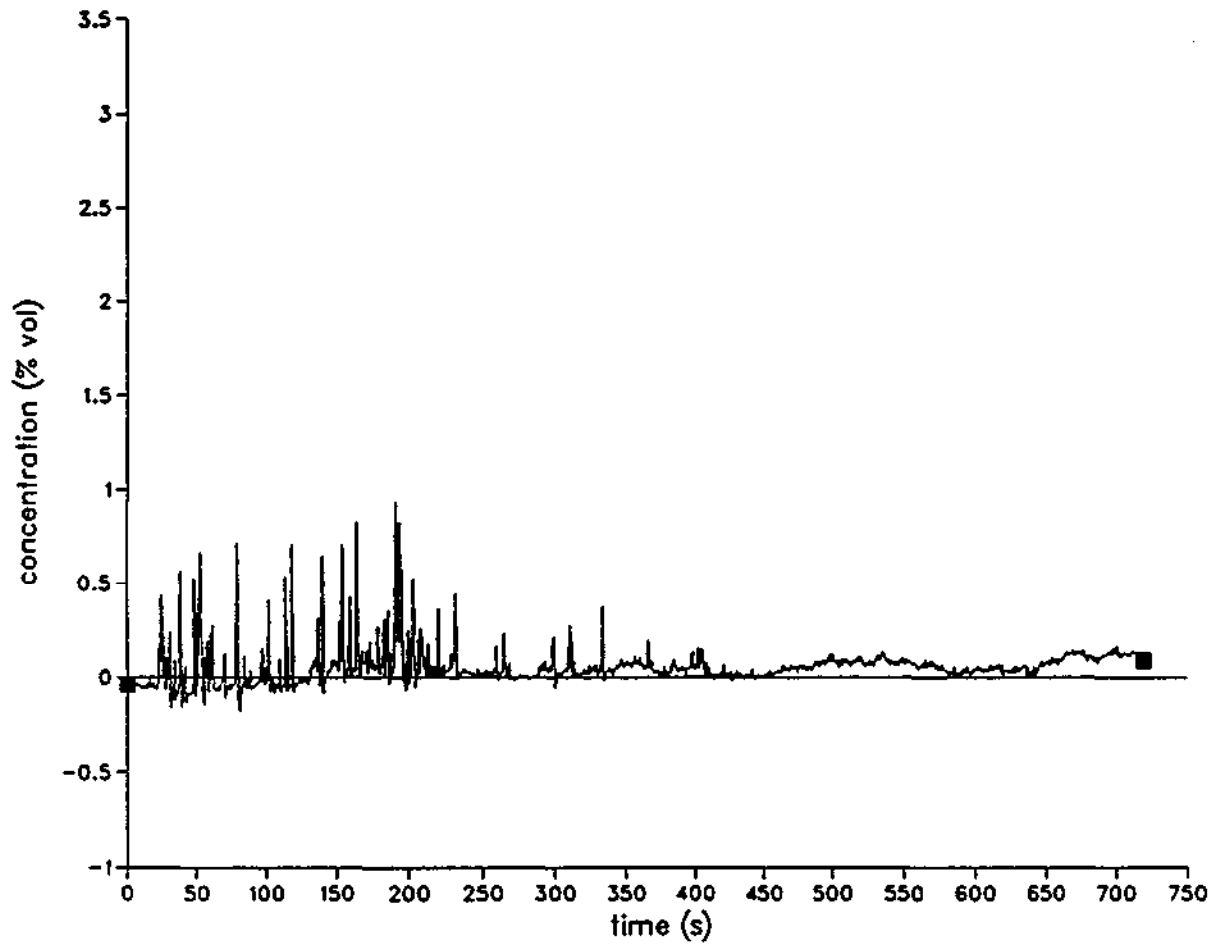
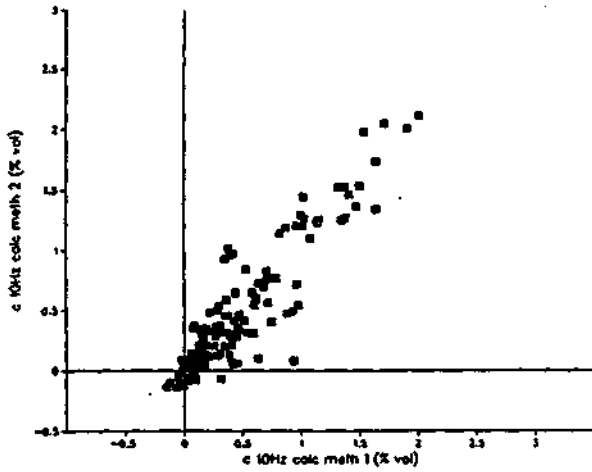
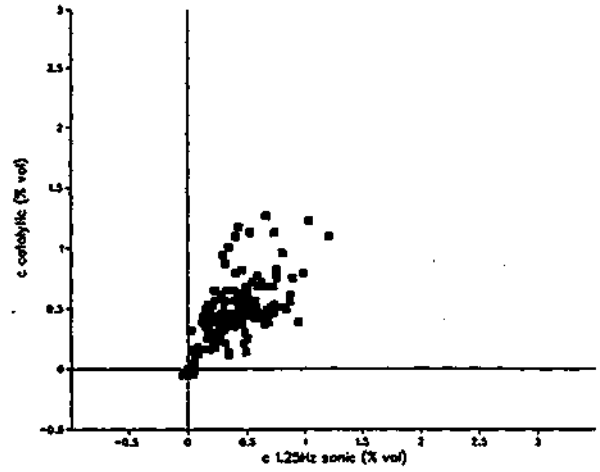


Figure 6 A typical fast sonic record from a height of 4m.

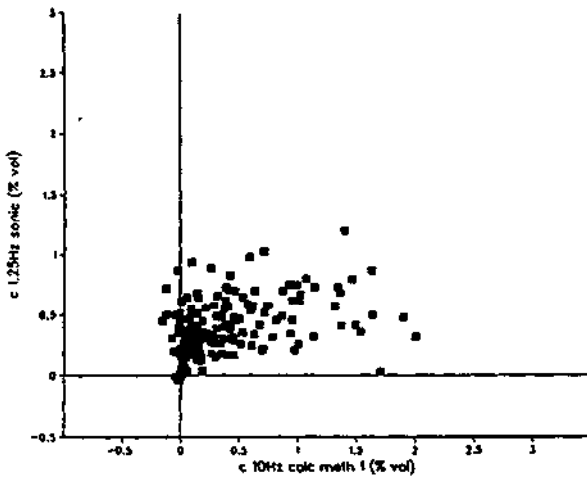
EEC55 mast3 height 2m,10Hz: calc meth2 vs calc meth1



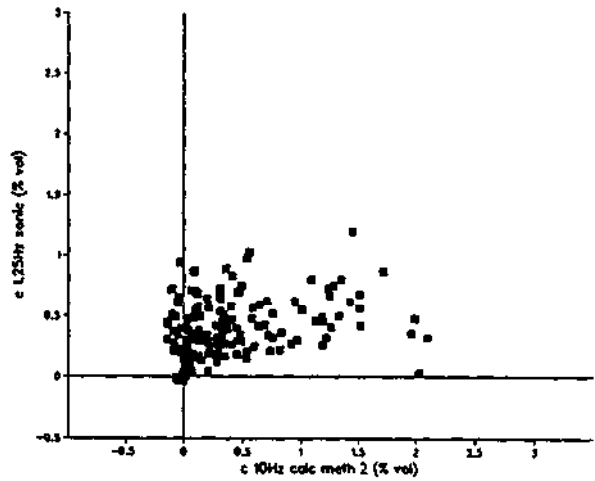
EEC55 mast3 height 2m,catalytic vs 1.25Hz sonic



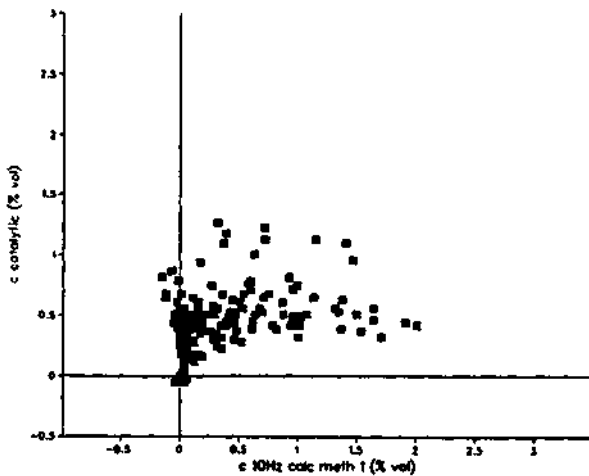
EEC55 mast3 height 2m,1.25Hz sonic vs 10Hz calc meth1



EEC55 mast3 height 2m,1.25Hz sonic vs 10Hz calc meth2



EEC55 mast3 height 2m,catalytic vs 10Hz calc meth1



EEC55 mast3 height 2m,catalytic vs 10Hz calc meth2

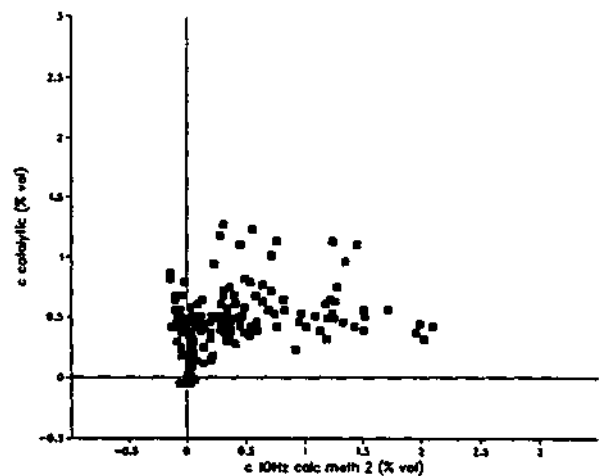


Figure 7 Scatter diagrams at one position in EEC 55 for all possible pairwise comparisons. (Refer to text and Table 3 for further details.)

### EEC56 mast 4 height 1m, dosage

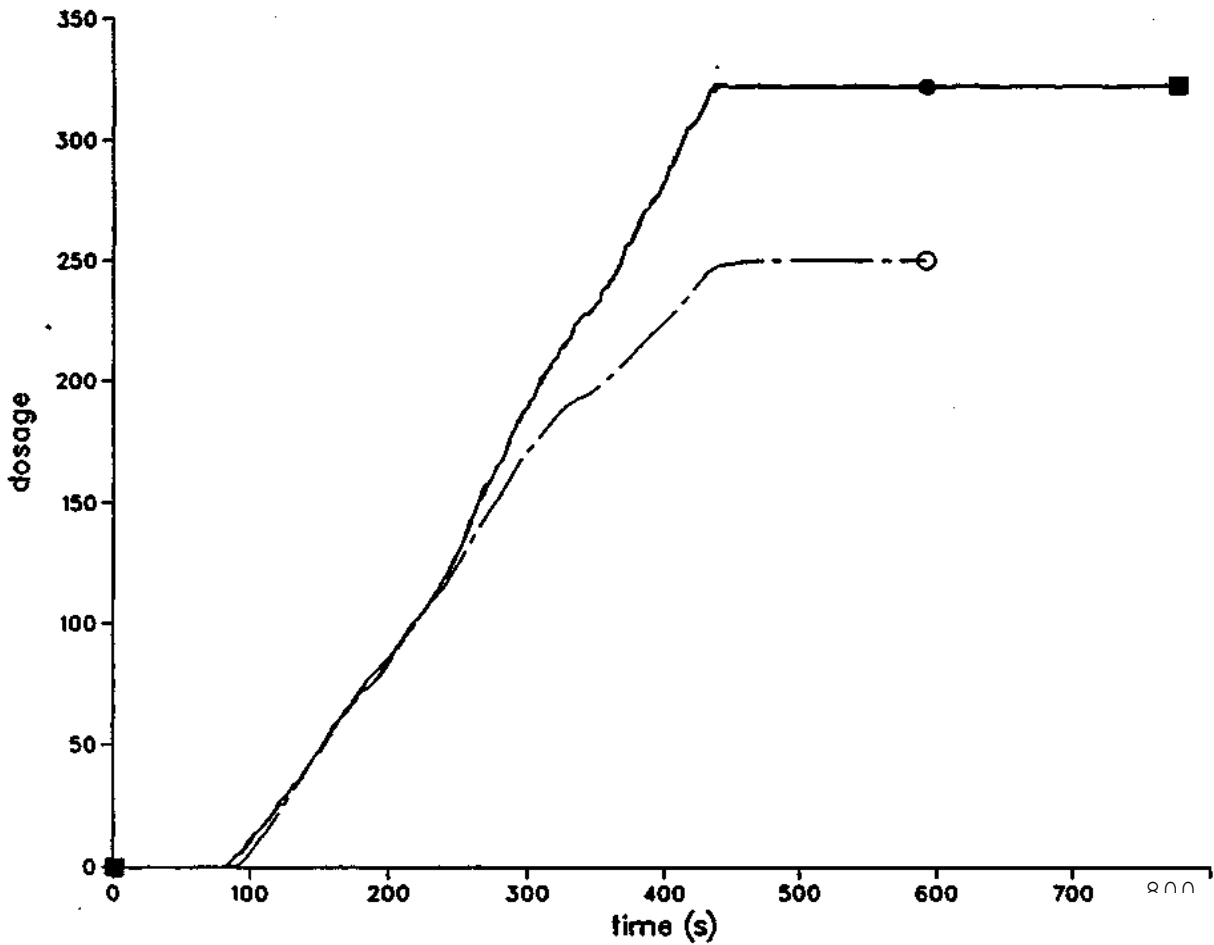
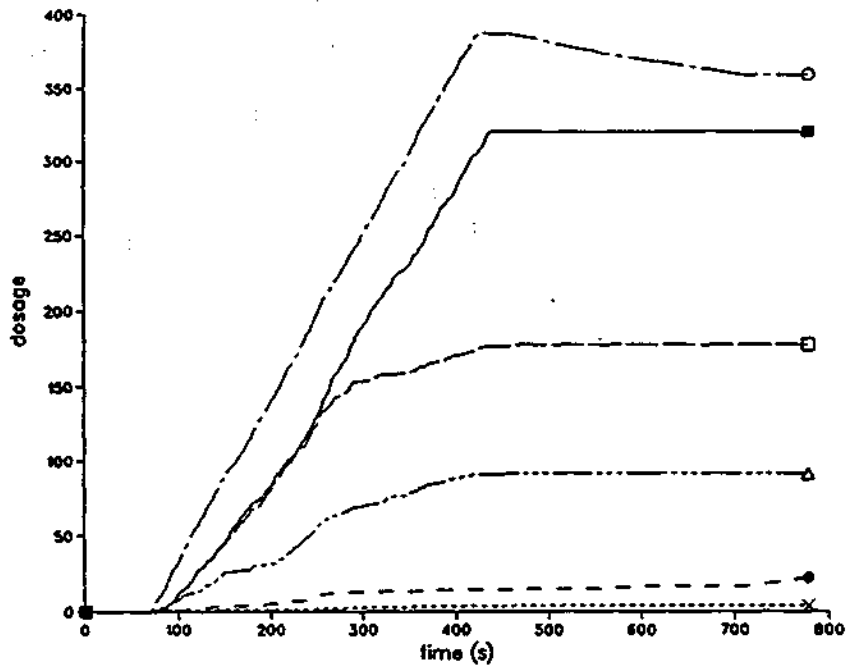


Figure 8 The dosages from the four measurement methods. Dosage is defined in equation (8). Symbols: ■ Fast sonics (both methods gave indistinguishable results for all time); ● 1.25 Hz sonic; ○ catalytic.

EEC56 dosages from 10Hz sonic (calc method 1)



EEC57 dosages from 10Hz sonic (calc method 1)

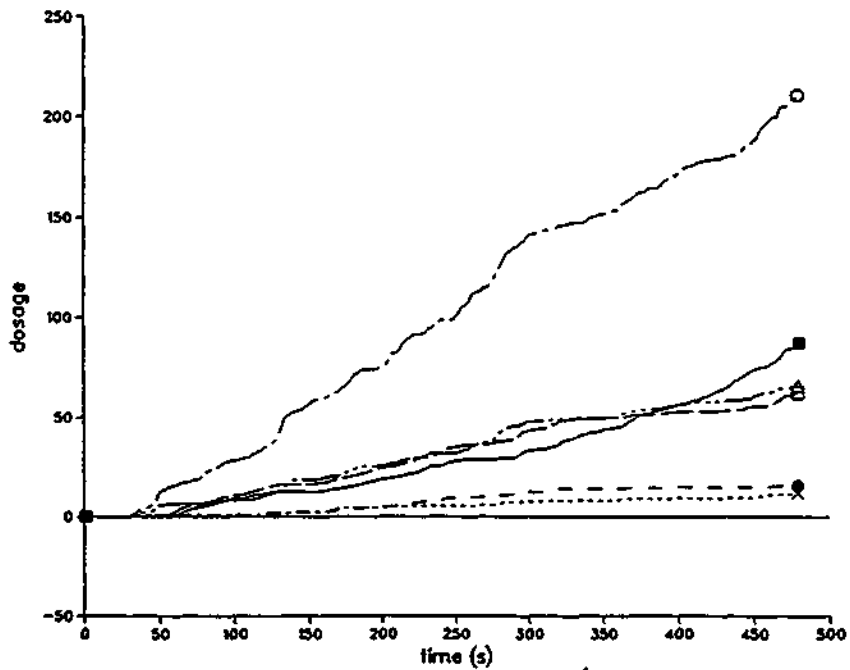


Figure 9 Dosages from (a) a jet release (EEC 56), (b) a cyclone release (EEC 57). Symbols: ■ mast 4 at 1m; □ mast 4 at 2m; ● mast 4 at 4m; o mast 3 at 1m; Δ mast 3 at 2m; X mast 3 at 4m.

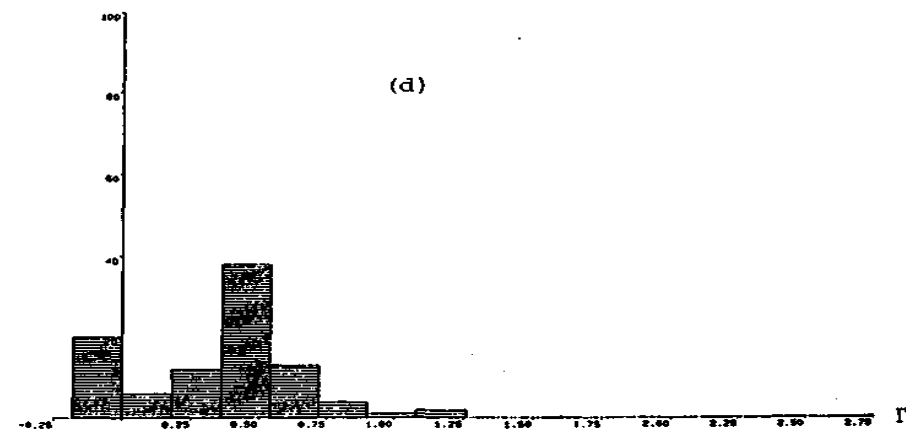
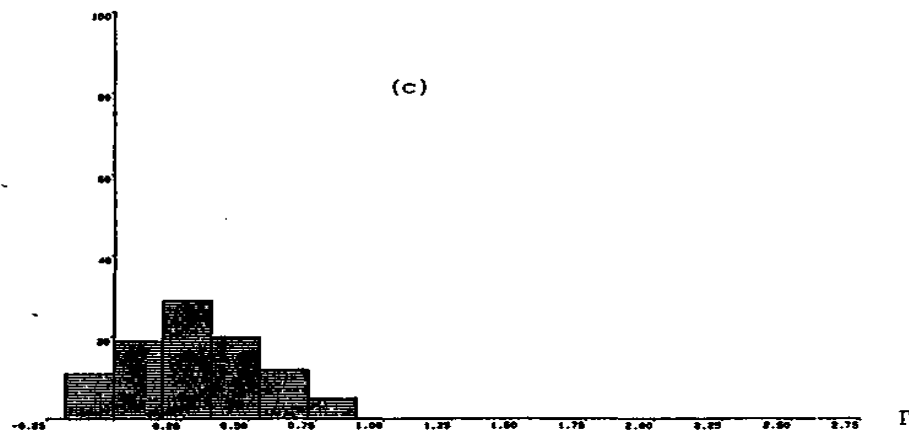
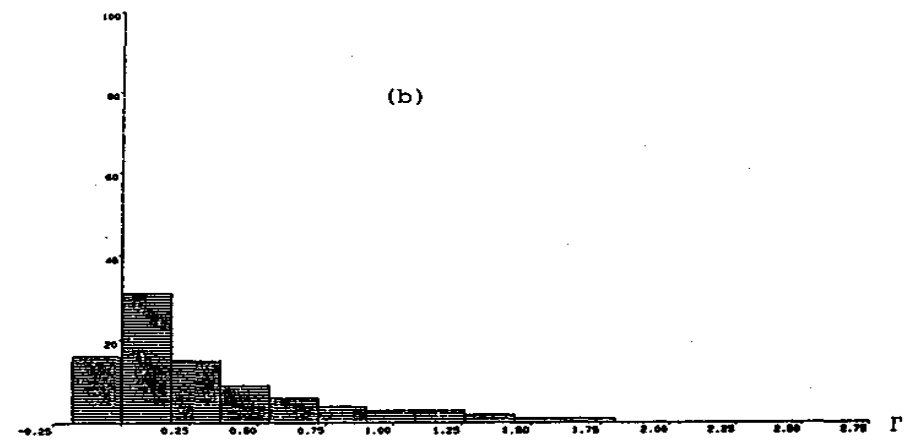
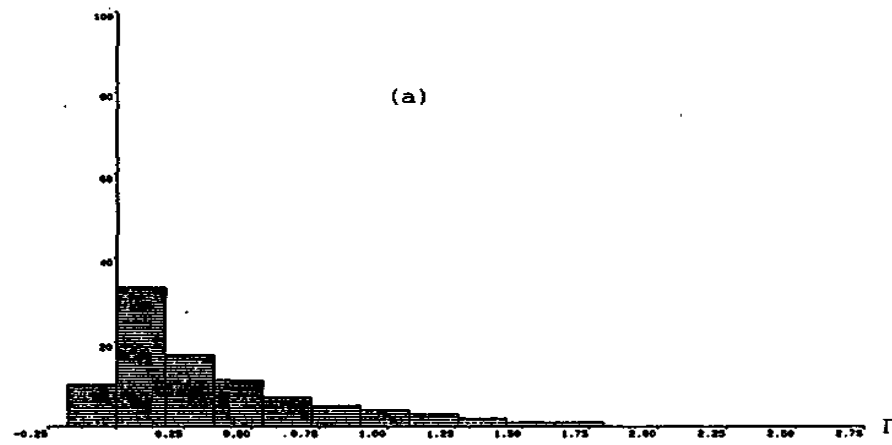


Figure 10 Histograms from EEC 55, mast 3 at 2m. (a) 10Hz sonic, method 1; (b) 10Hz sonic, method 2; (c) 1.25Hz sonic; (d) catalytic. The vertical axis is relative frequency (as a percentage).

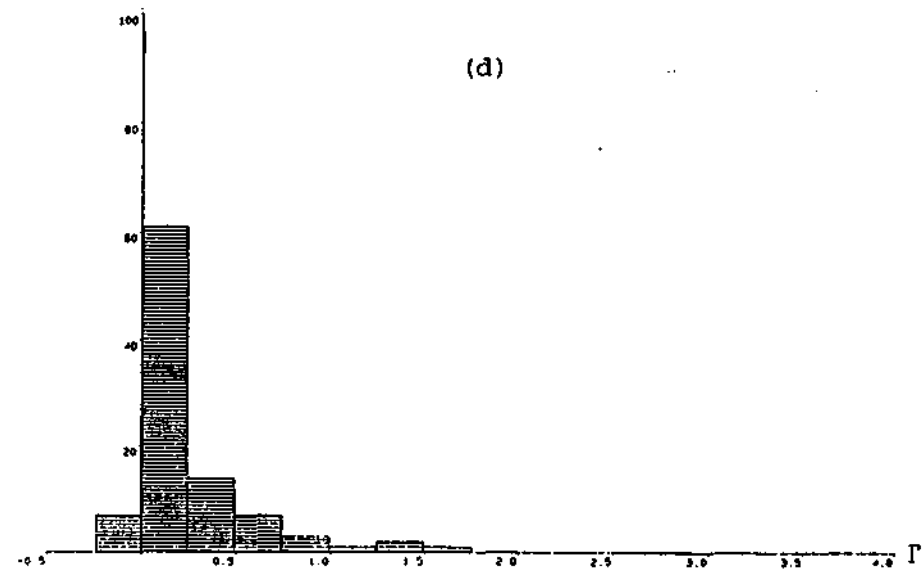
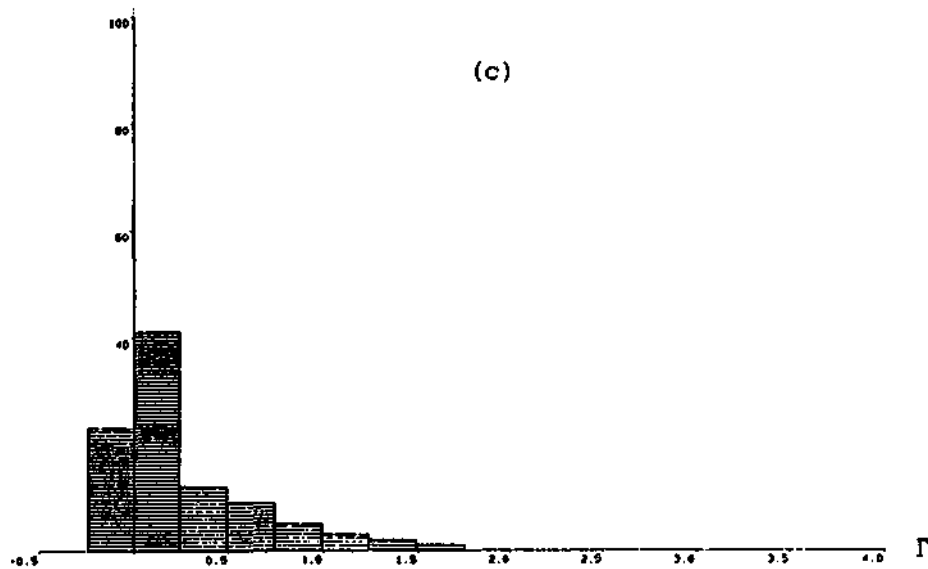
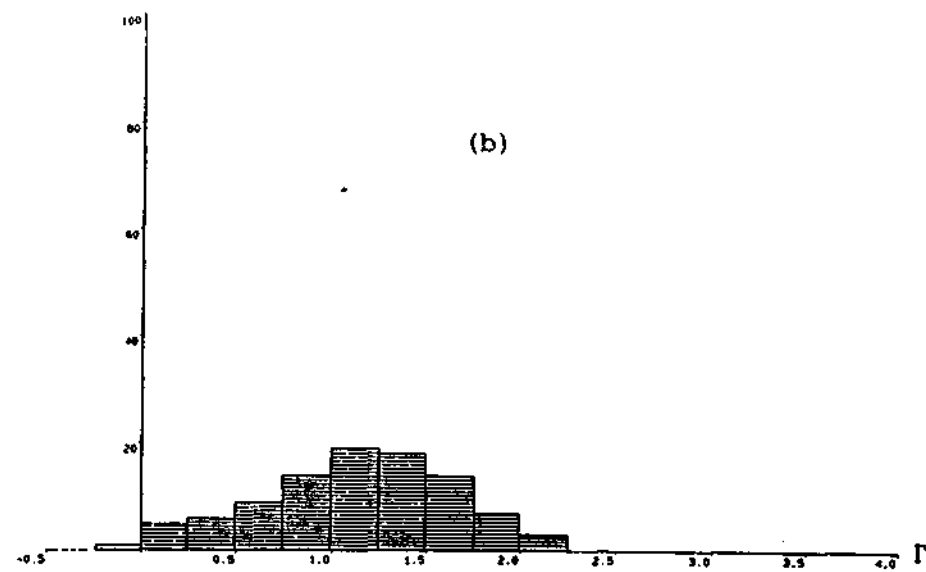
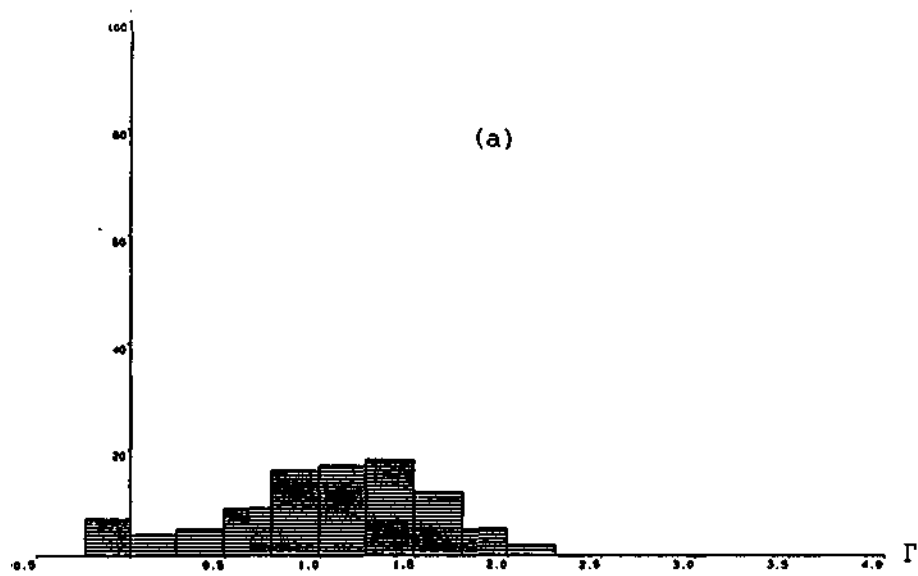
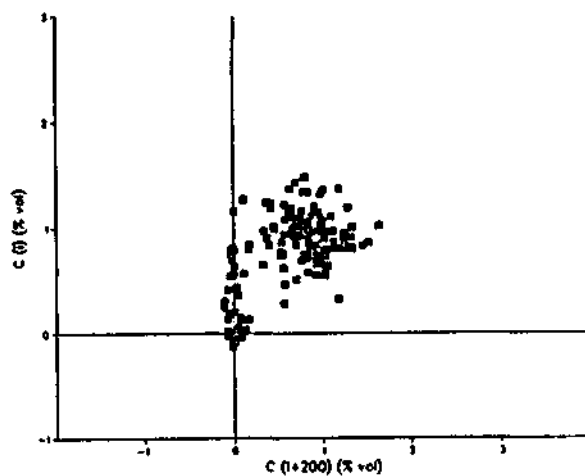


Figure 11 Histograms from EEC 56 at mast 4 taken with 10Hz sonic, method 1. (a) lm, with fence; (b) lm, without fence; (c) 2m, with fence; (d) 2m, without fence.

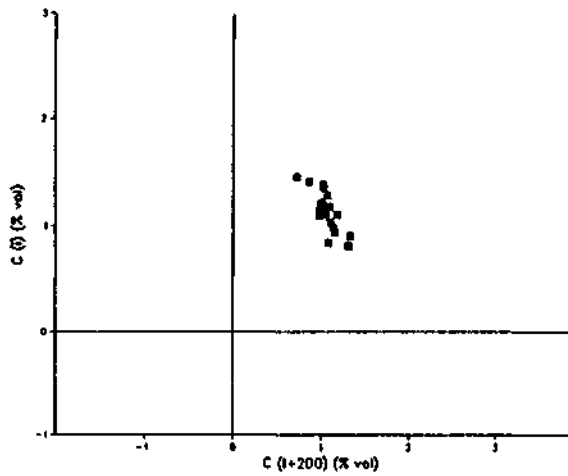
EEC55 mos!4 height 1m,10Hz sonlc(colc melh l),before fence wenl down

EEC55 mos!4 heighl 1m.10Hz sonic(colc melh l),during fence going down

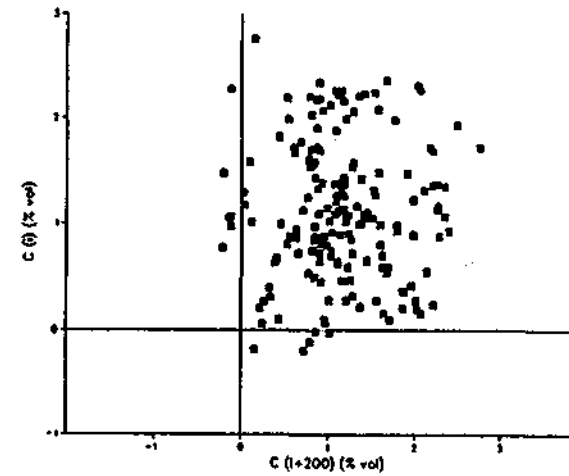
EEC55 mos!4 height 1m,10H2 sonic(cotc meth l),ofler fence went down



(a)



(b)



(c)

Figure 12 Plots of  $r(t) = C(i)$  -ordinate-versus  $r(t + 20s) = C(i + 200)$  -abscissa-for three different time regimes in EEC 55. (See text for further details.)

ALGORITHM FOR DETECTING WHEN FENCE REMOVED

- For each second during a run, determine:

$m(t)$  = mean of concentration from release at  $t = 0$ ;

$s(t)$  = standard deviation of concentration.

- Calculate

$$F(t) = \frac{s(t) - s(t-1)}{s(t-1)} - 5 \frac{s(t) - s(t-1)}{m(t-1)},$$

(where  $m(t-1)$  is value of  $m$  one second before  $t$  etc.).

- Find first value of  $t$ , say  $t = T$ , for which

$$|F(t)| > 100 \text{ and } m(t) > 0.5.$$

- Fence is removed at  $t = T$ .

The figures illustrate that this produces results that are closer than 1 second to values recorded on data tapes. Figure 13(c) is an expanded version of the relevant section of Figure 13(b).

(a)

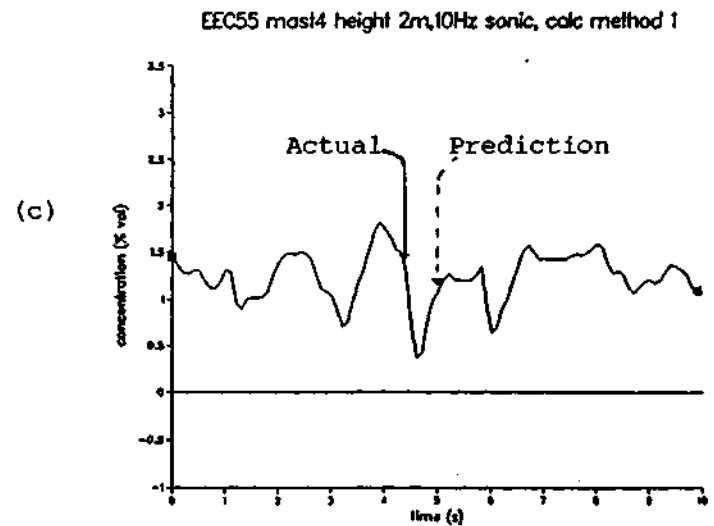
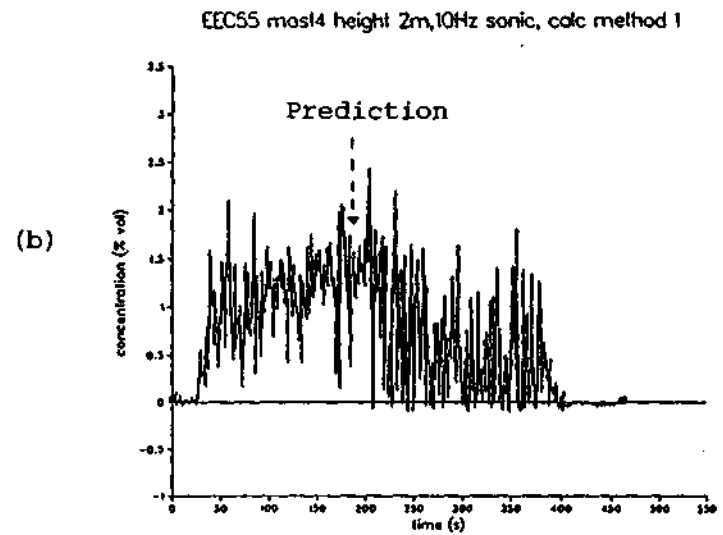


Figure 13



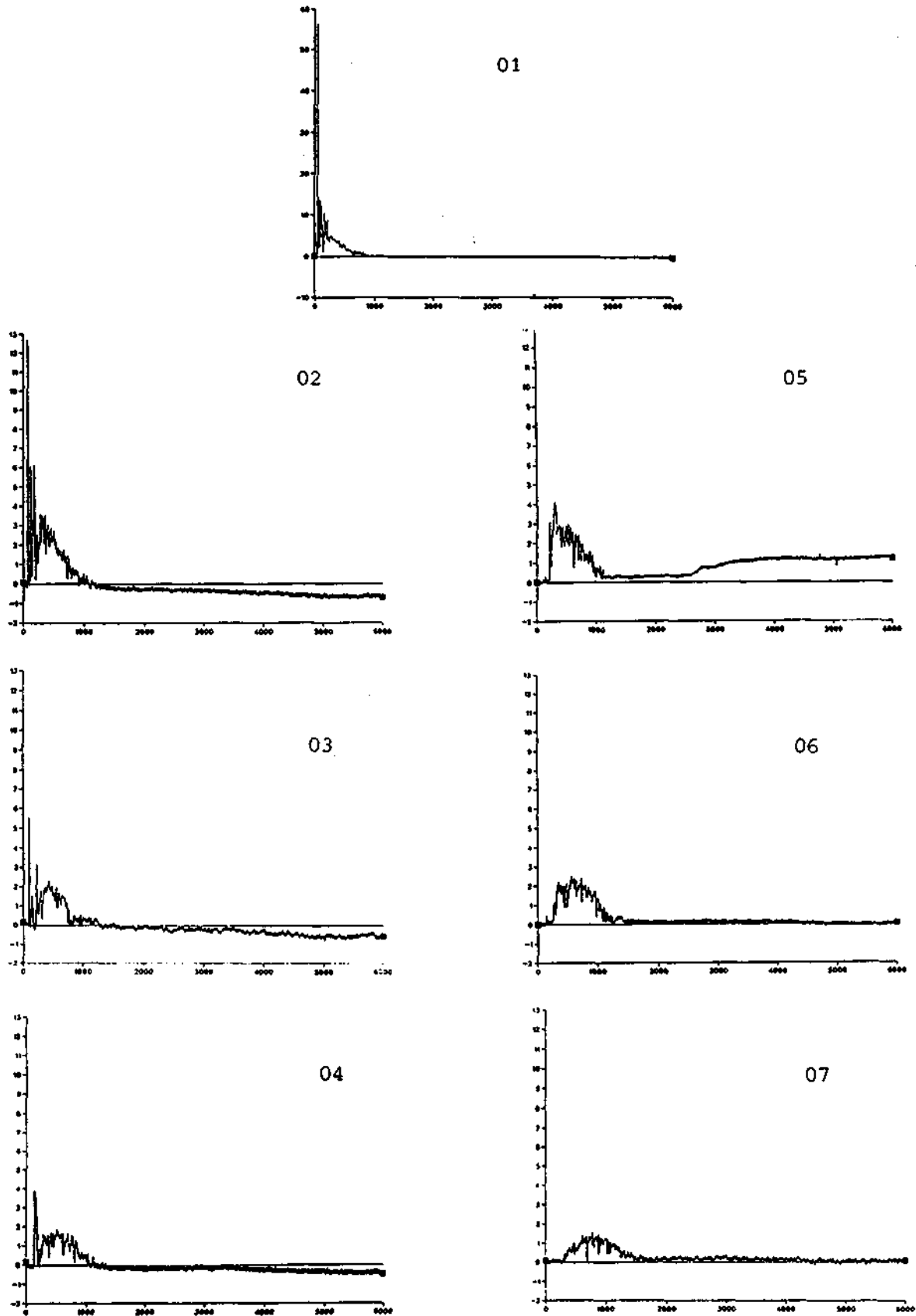
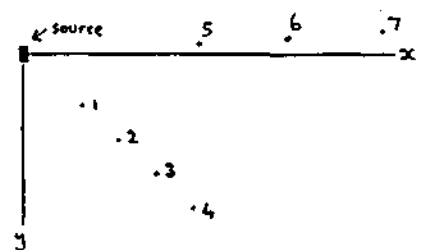
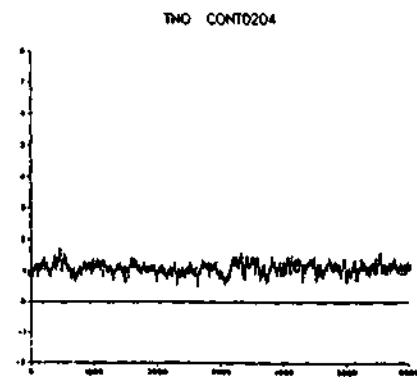
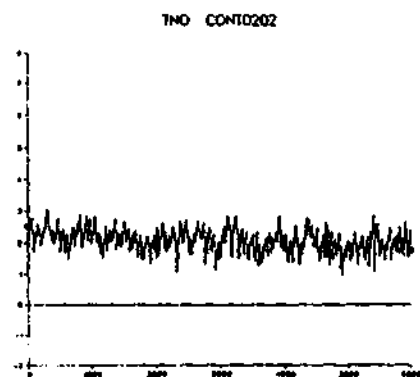
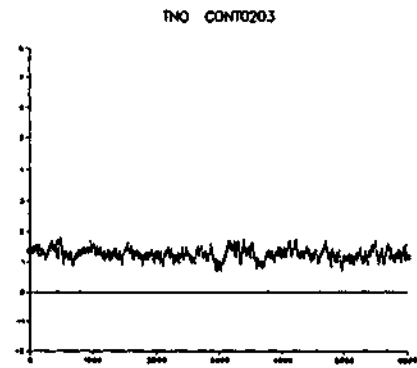
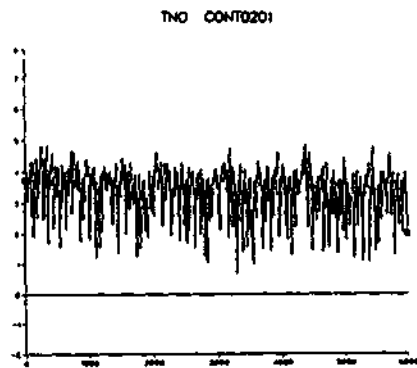
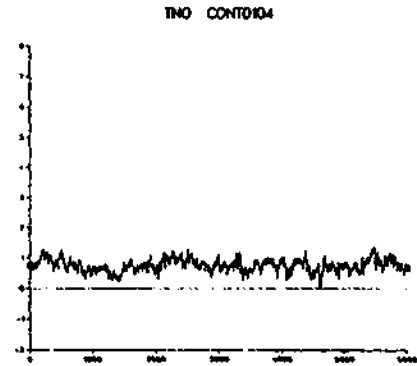
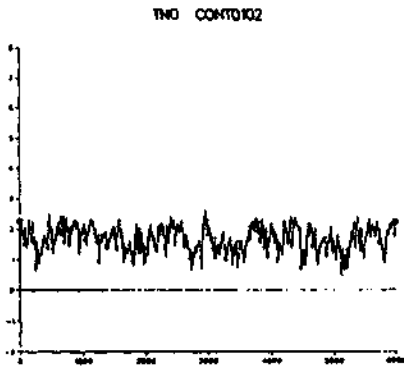
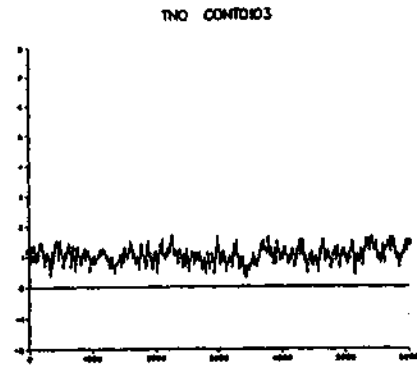
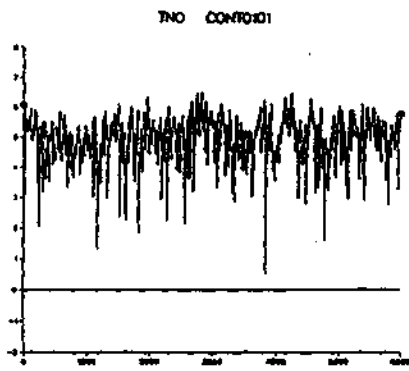


Figure 14 TNO instantaneous releases. Each figure is labelled with its location (see Table 5 and sketch on right). Note that the vertical scale for 01 is different from that for 02 - 07 inclusive.





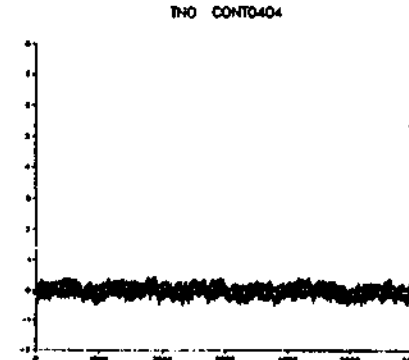
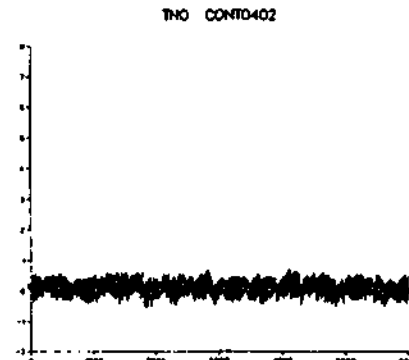
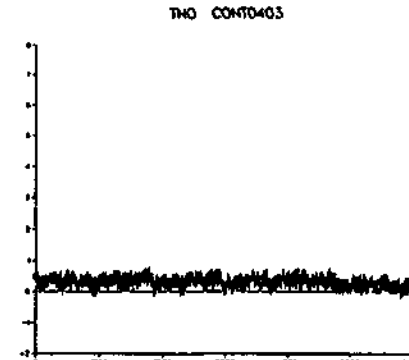
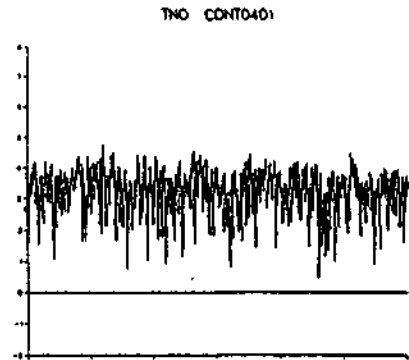
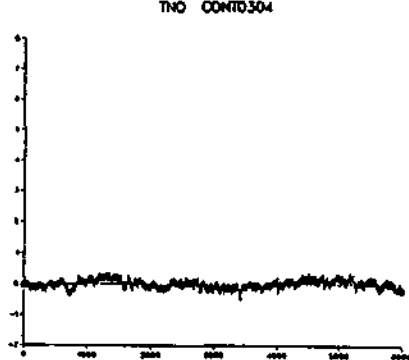
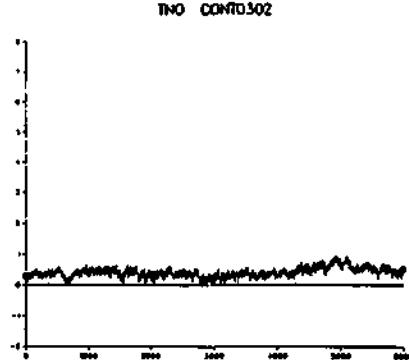
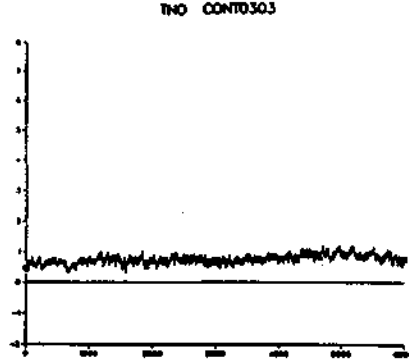
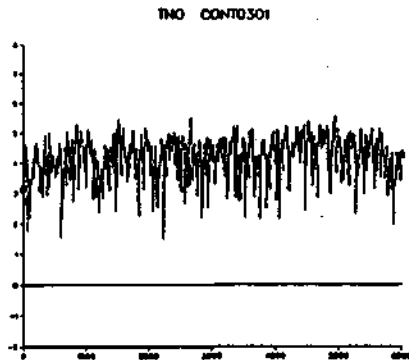


Figure 15 - Page two of three

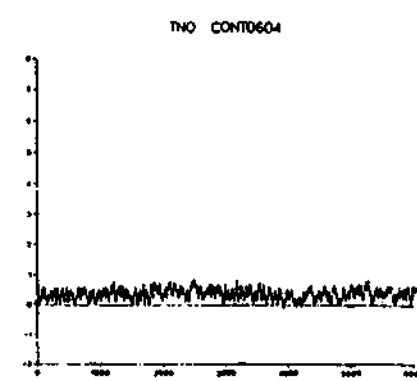
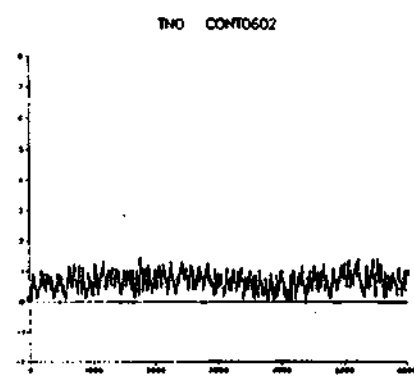
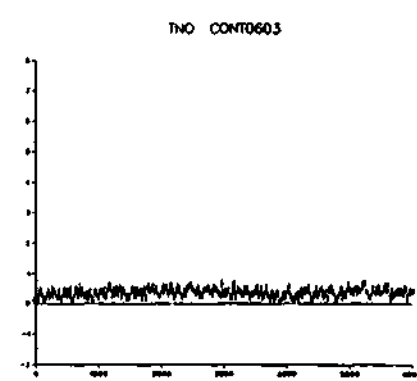
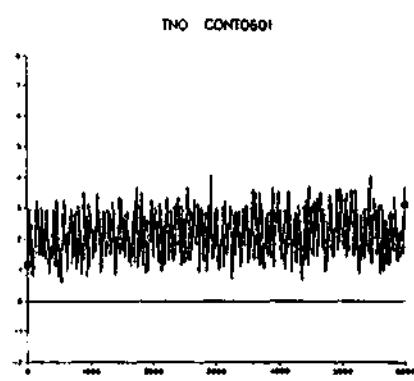
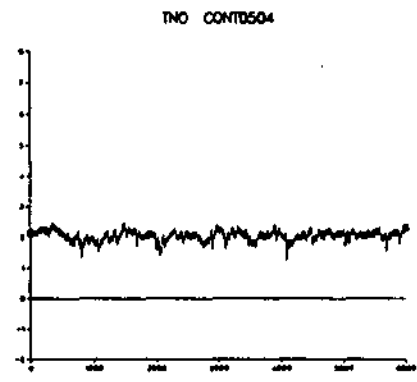
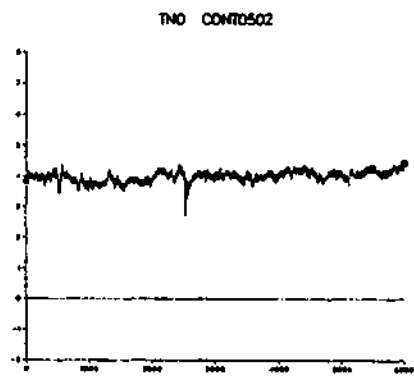
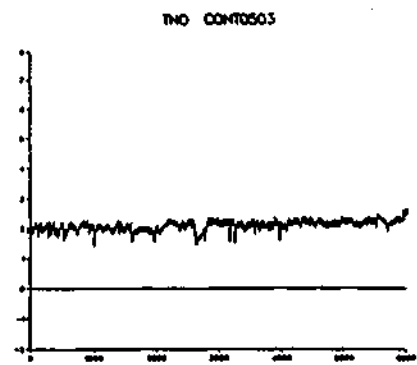
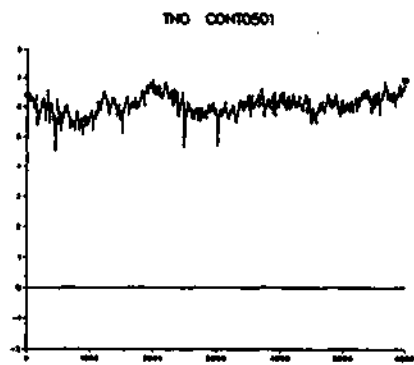


Figure 15 - Page three of three

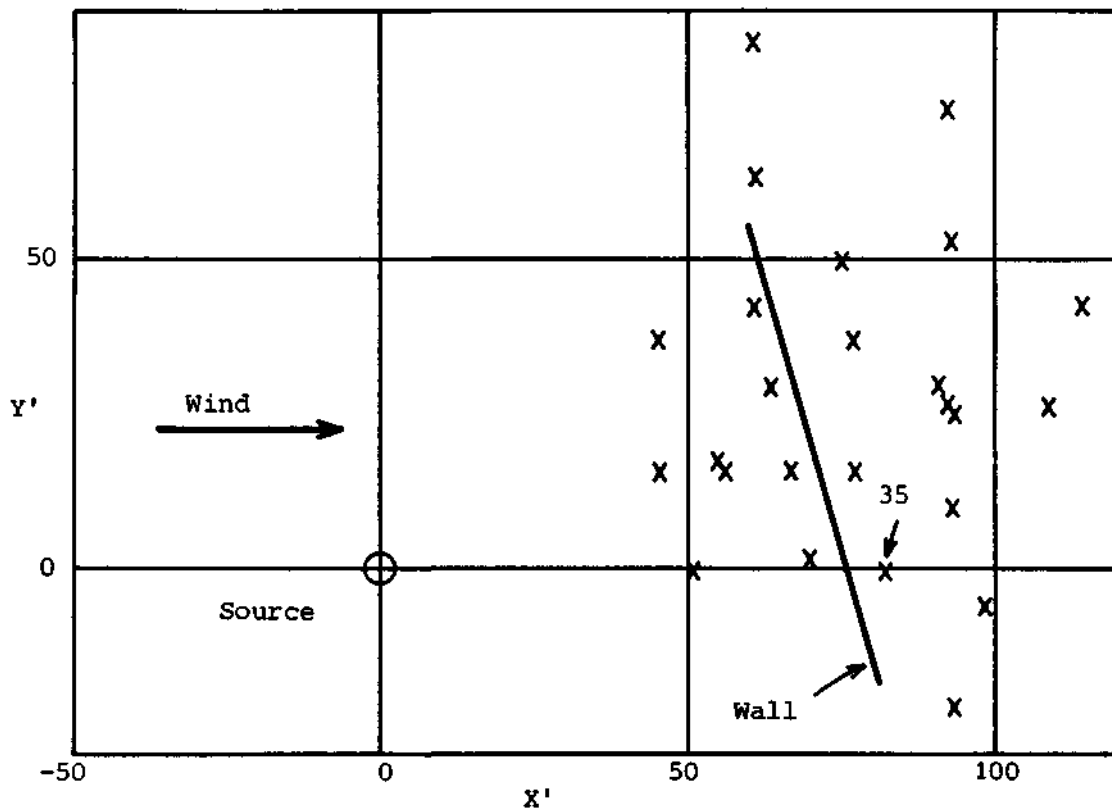
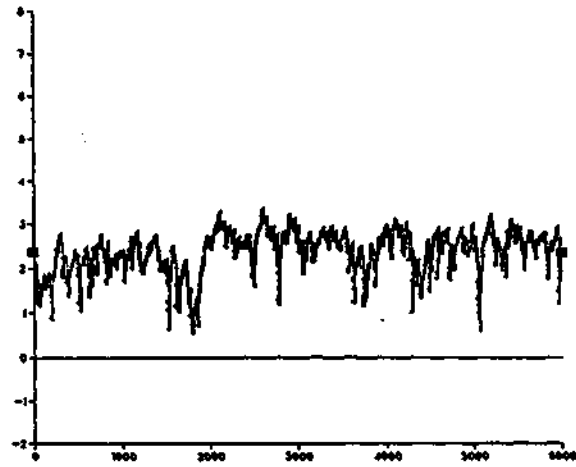
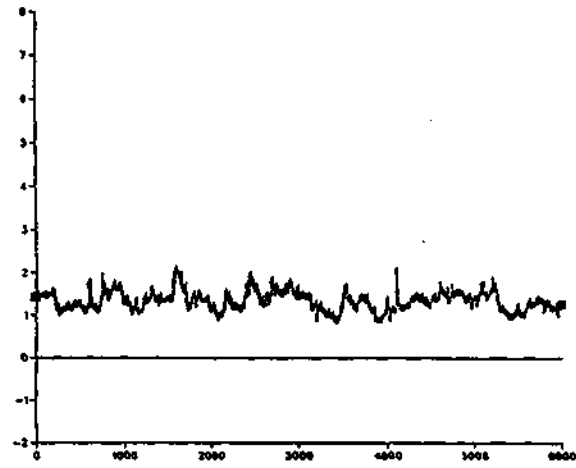


Figure 16            Layout of EEC 57.  $x', y'$  are measured in units of  $L_{cc}$ . X denotes sensor positions in EEC 57 (some catalytic, some infrared, some sonic, some more than one of these). The TNO results shown in Figures 17 and 18 were taken at position 35 in the wind-tunnel simulation of EEC 57.

TNO TUV0301



TNO TUV0302



TNO TUV0303

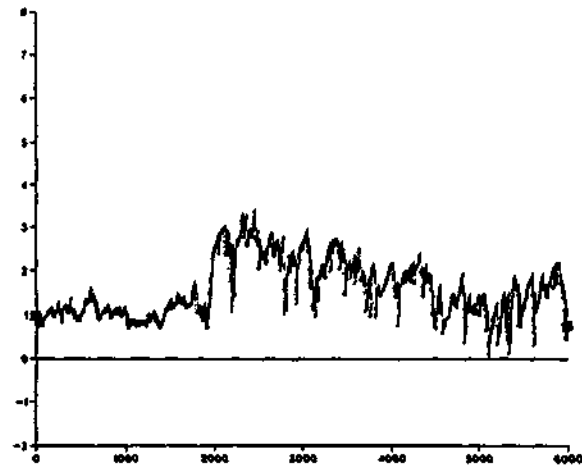
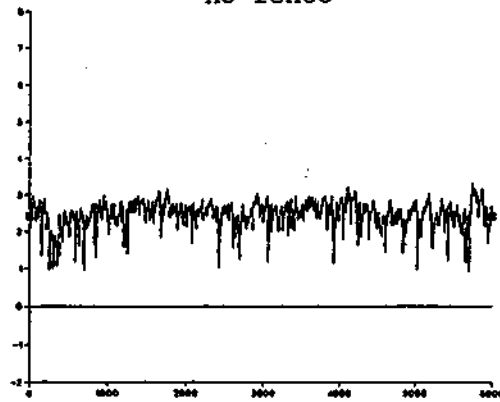
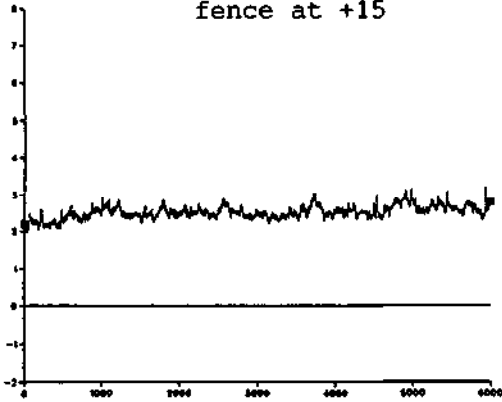


Figure 17

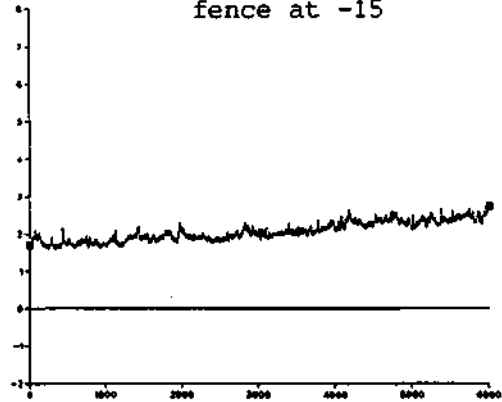
TNO TUV1201  
no fence



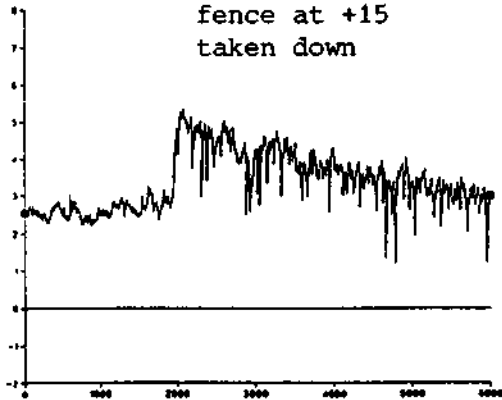
TNO TUV1202  
fence at +15



TNO TUV1203  
fence at -15



TNO TUV1204  
fence at +15  
taken down



TNO TUV1205  
fence at -15  
taken down

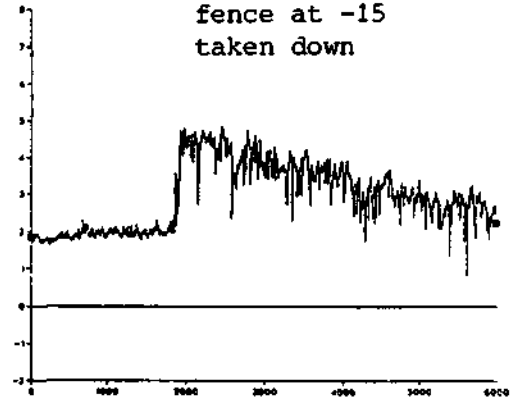


Figure 18

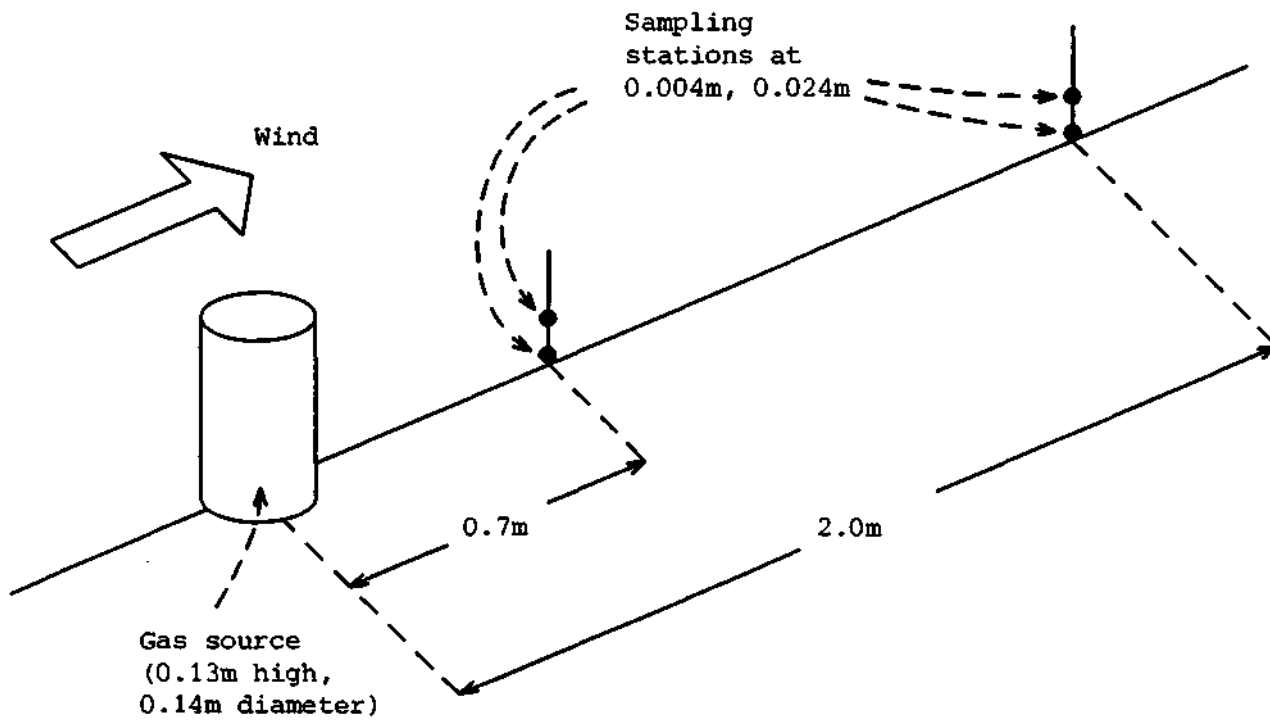


Figure 19 Layout for WSL experiments.



WSL Ri=10 (70,0,0.4) n=50 TYPICAL REPETITION

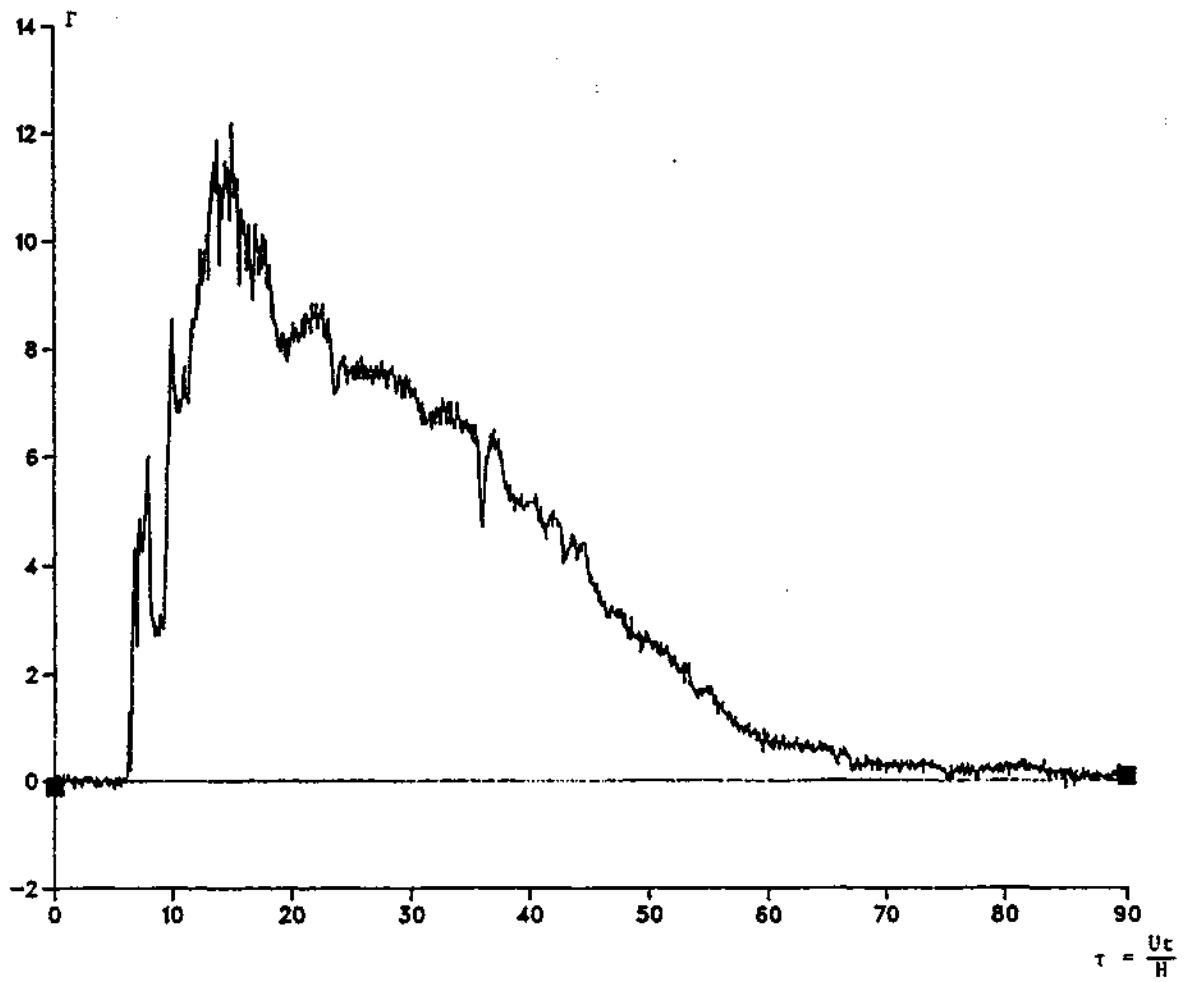


Figure 20 A typical time-series for the WSL data.

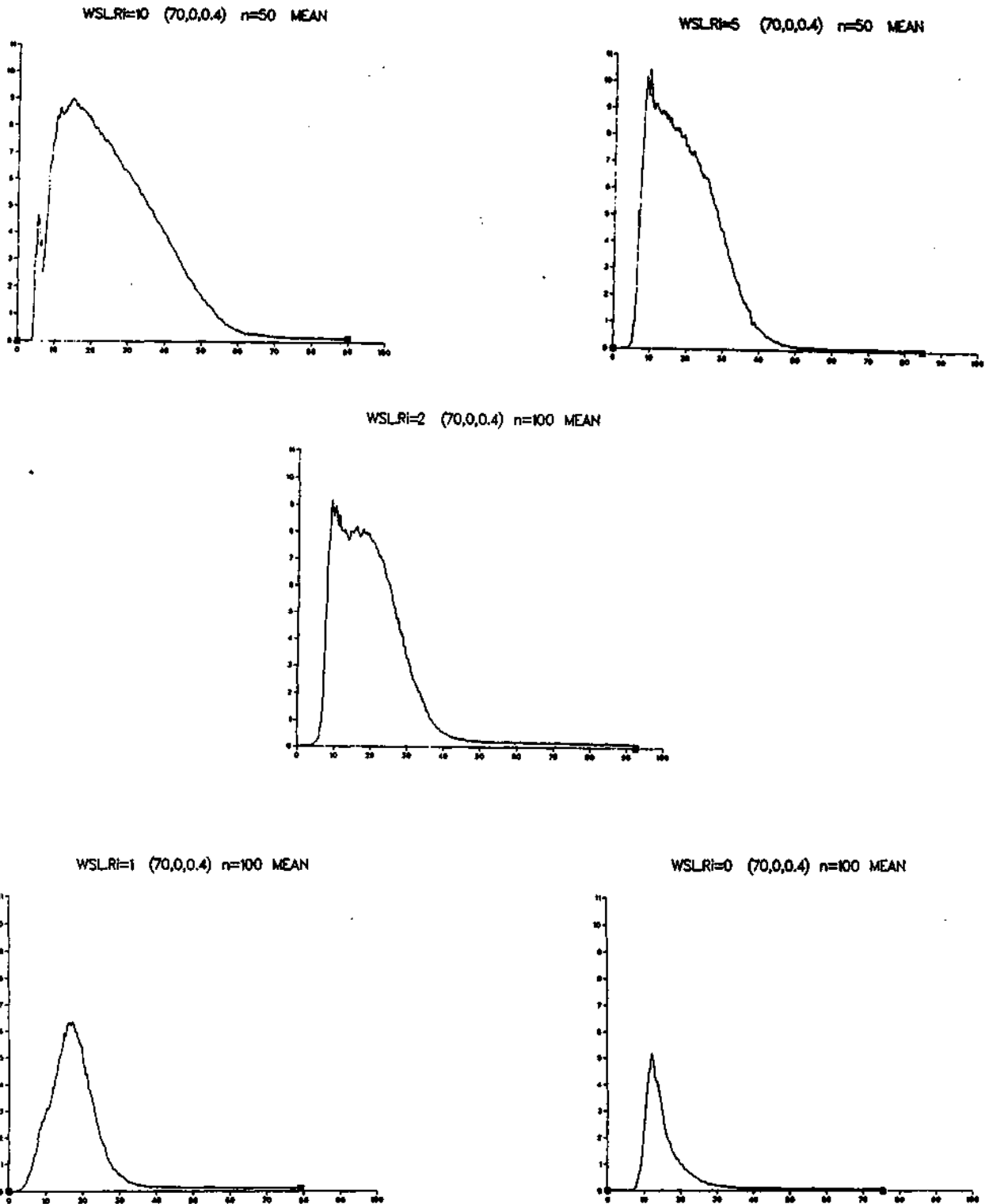


Figure 21 Graphs of  $m(t)$  as percentages (ordinate) versus  $\tau = Ut/H$  (abscissa) taken at the station 0.7m downwind and 0.004m from the wind-tunnel floor.

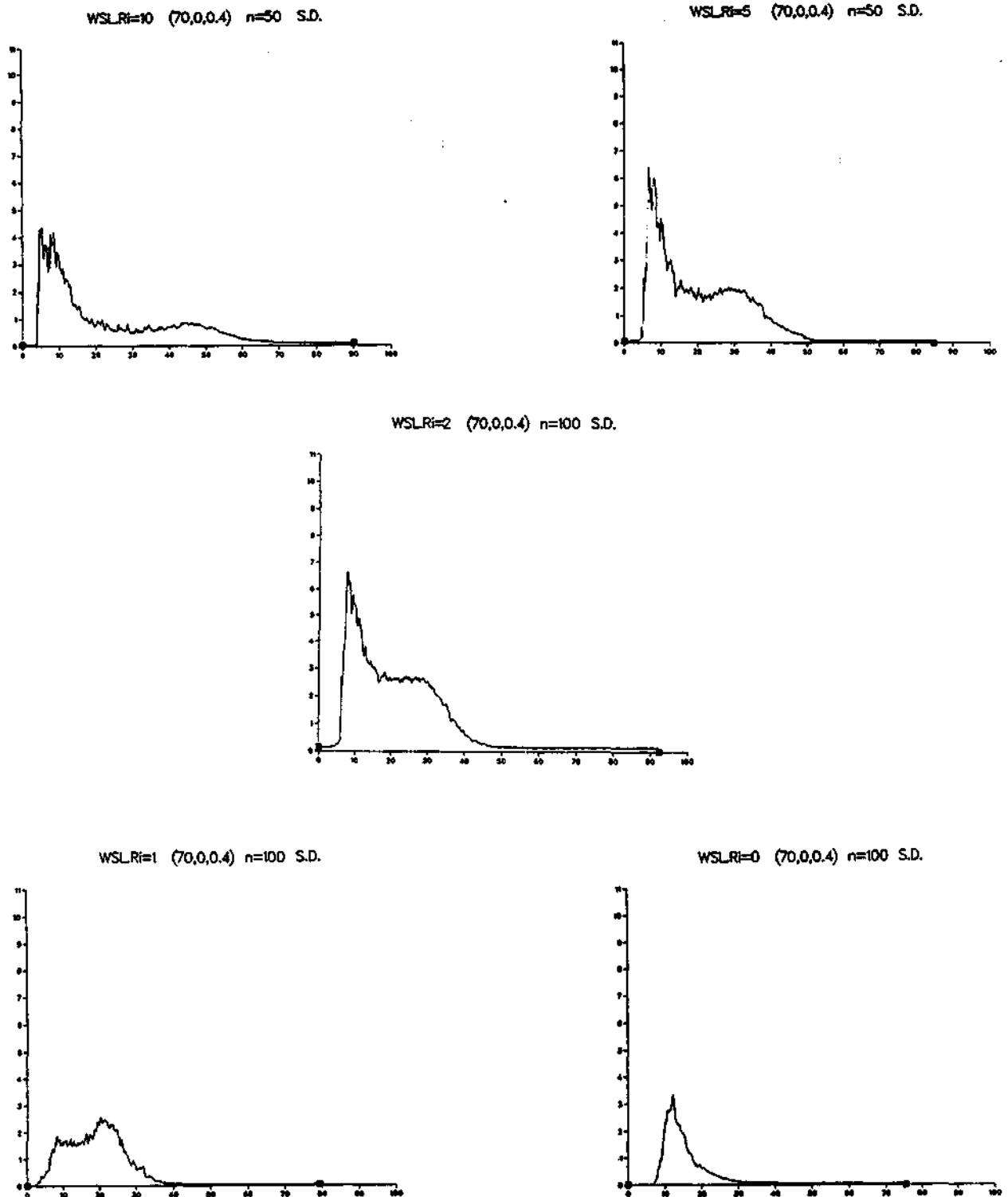


Figure 22 Graphs of  $s(t)$  as percentages (ordinate) versus  $\tau = Ut/H$  (abscissa) taken at the station 0.7m downwind and 0.004m from the wind-tunnel floor.

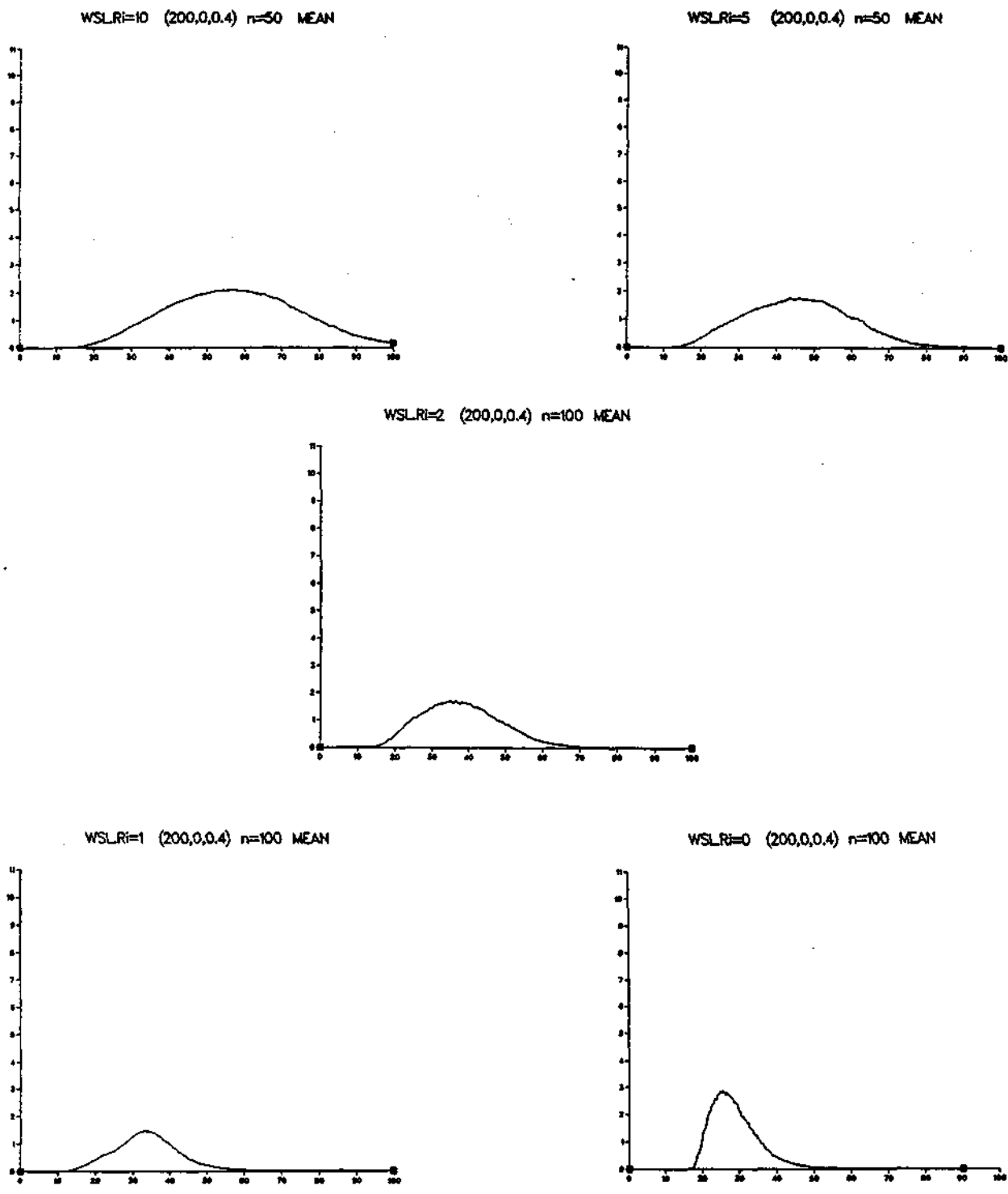


Figure 23 Graphs of  $m(t)$  as percentages (ordinate) versus  $\tau = Ut/H$  (abscissa) taken at the station 2.0m downwind and 0.004m from the wind-tunnel floor.

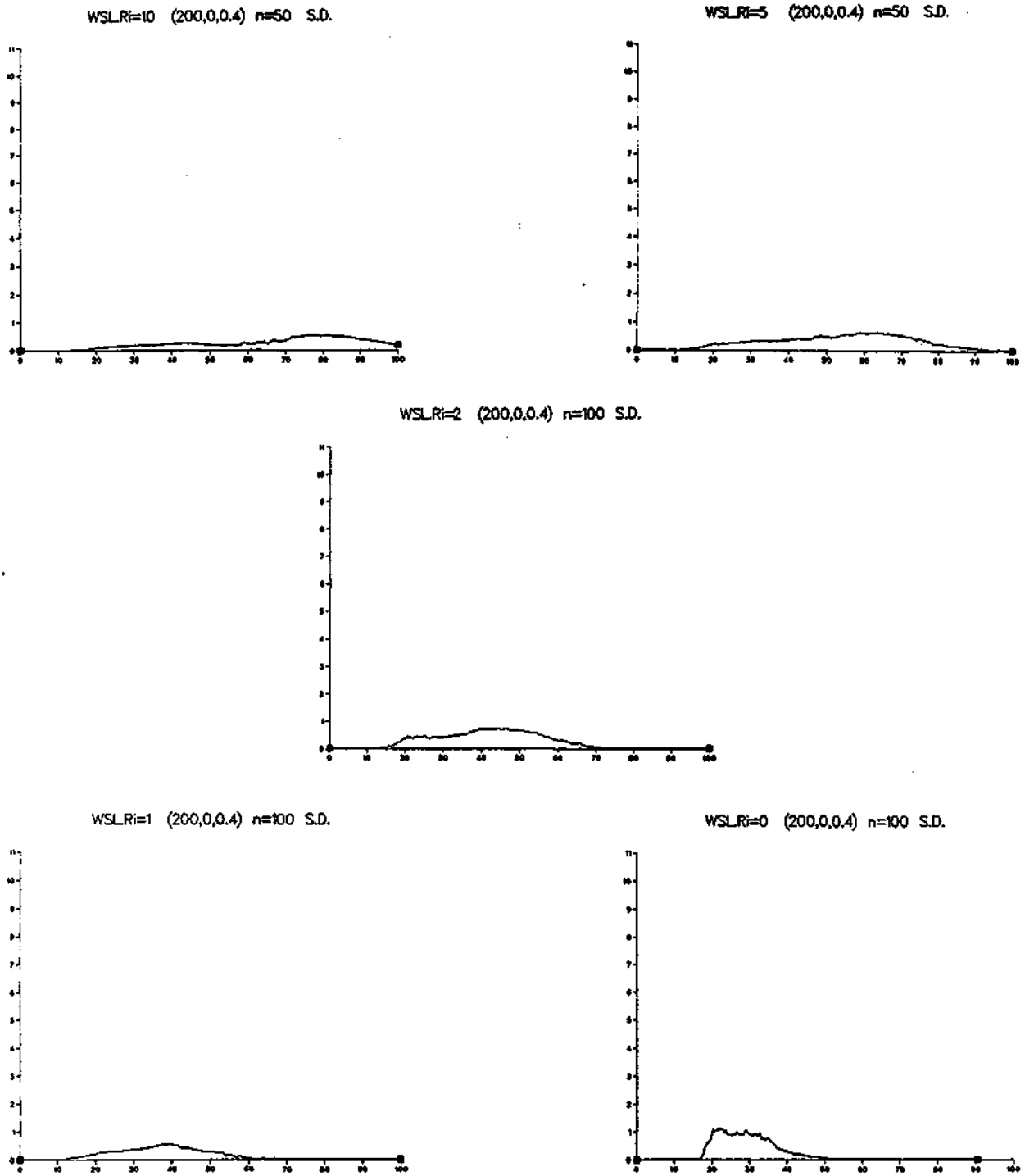
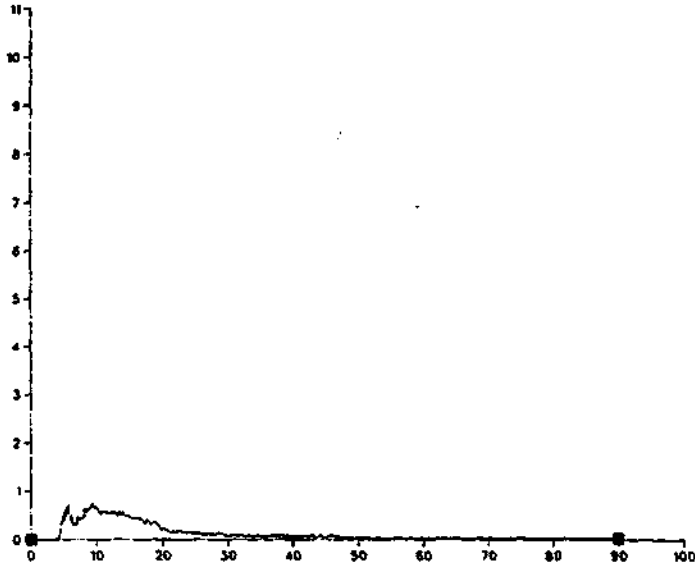


Figure 24 Graphs of  $s(t)$  percentages (ordinate) versus  $\tau = Ut/H$  (abscissa) taken at the station 2.0m downwind and 0.004m from the wind-tunnel floor.

WSL<sub>Ri</sub>=10 (70,0,2.4) n=50 MEAN



WSL<sub>Ri</sub>=0 (70,0,2.4) n=100 MEAN

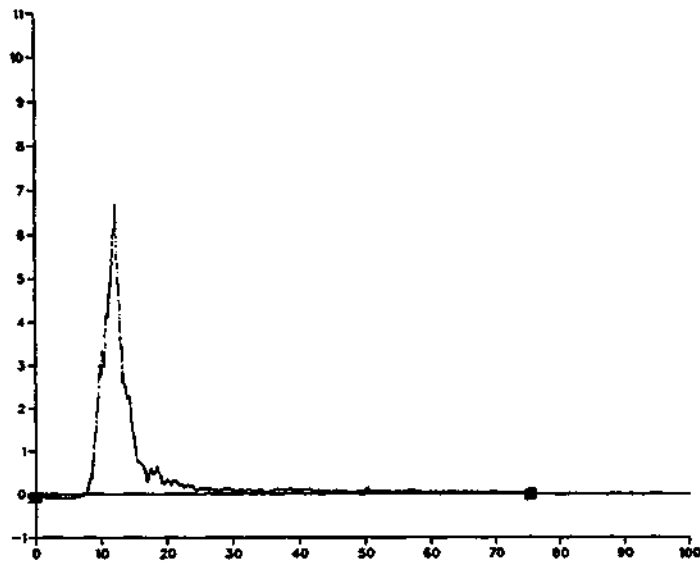
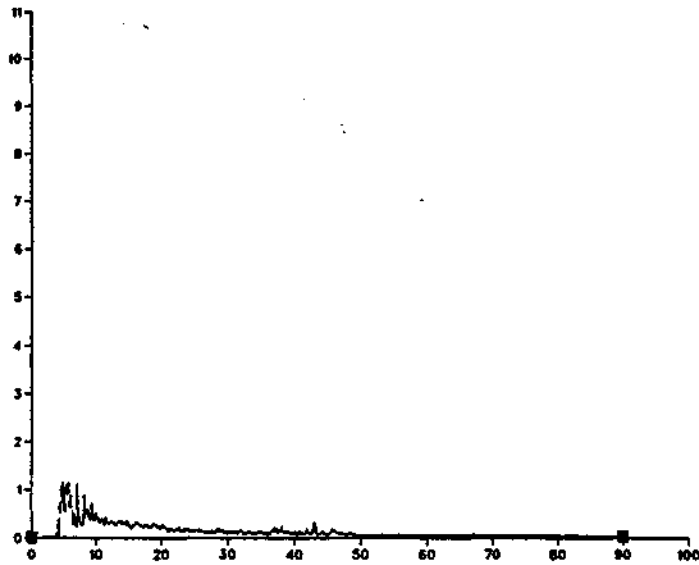


Figure 25 Graphs of  $m(t)$  as percentages (ordinate) versus  $\tau = Ut/H$  (abscissa) taken at the station 0.7m downwind and 0.024m from the wind-tunnel floor.

(Note that the vertical scales are not quite identical but it is nevertheless clear that the maximum value of  $m$  for  $Ri = 0$  is much greater than that for  $Ri = 10$ .)

WSL.Ri=10 (70,0,2.4) n=50 S.D.



WSL.Ri=0 (70,0,2.4) n=100 S.D.

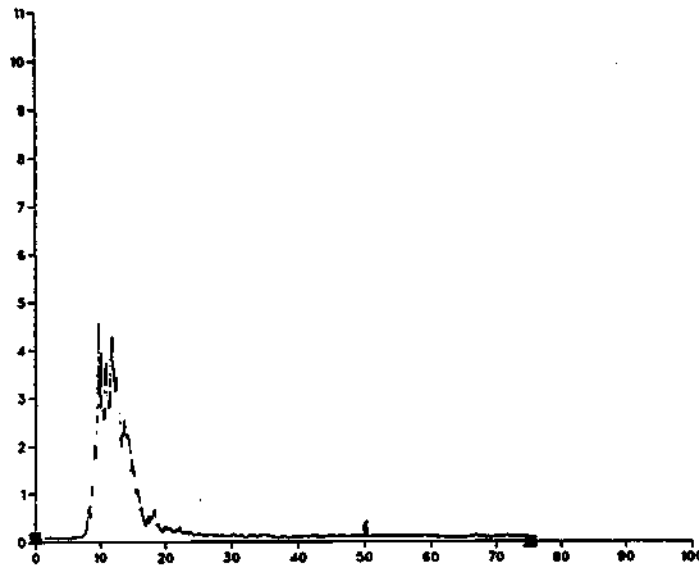
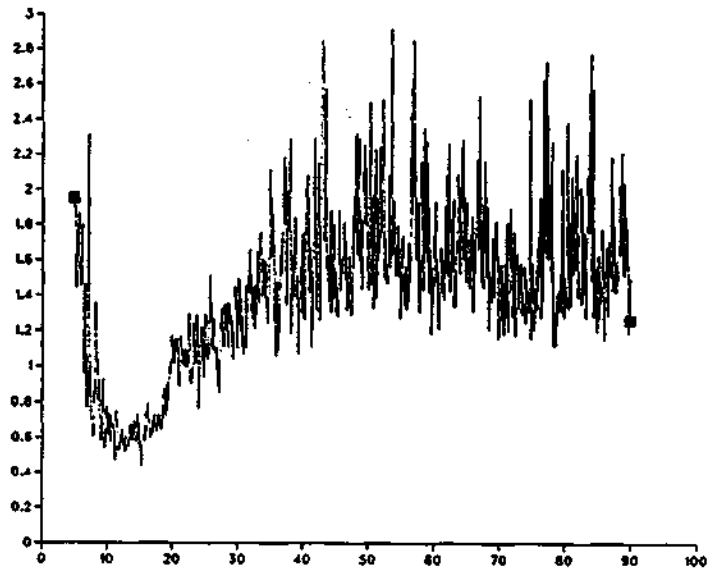


Figure 26 Graphs of  $s(t)$  as percentages (ordinate) versus  $\tau = Ut/H$  (abscissa) taken at the station 0.7m downwind and 0.024m from the wind-tunnel floor.

WSL.Ri=10 (70,0,2.4) n=50 INTENSITY



WSL.Ri=0 (200,0,0.4) n=100 INTENSITY

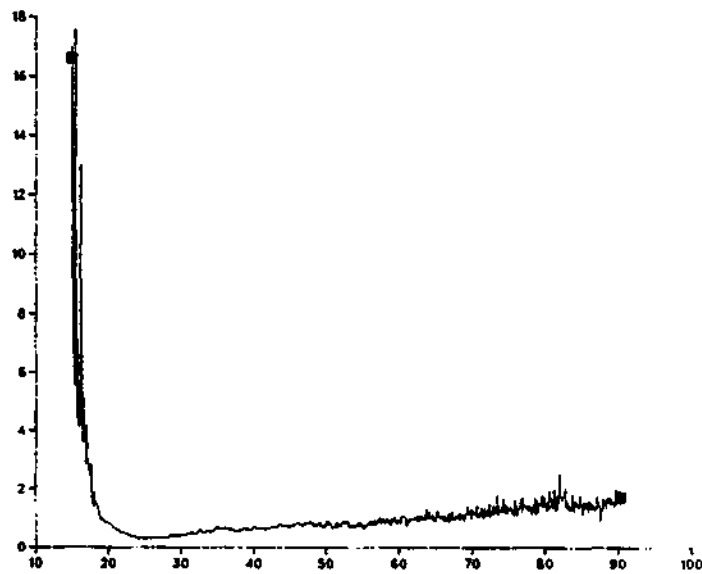


Figure 27 Two typical graphs of intensity =  $s/m$  versus  $\tau = Ut/H$ . Note that the vertical scales are different. The noise is mainly statistical and is obviously accentuated when  $m$  is small - see Figures 23 and 25.



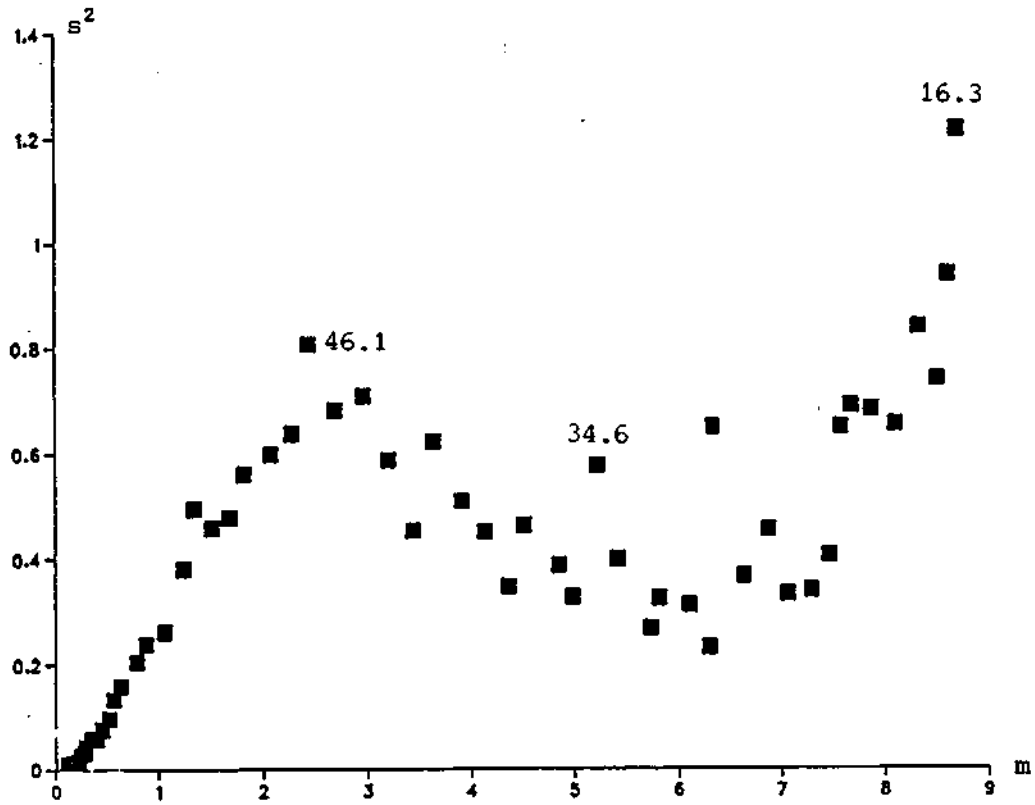
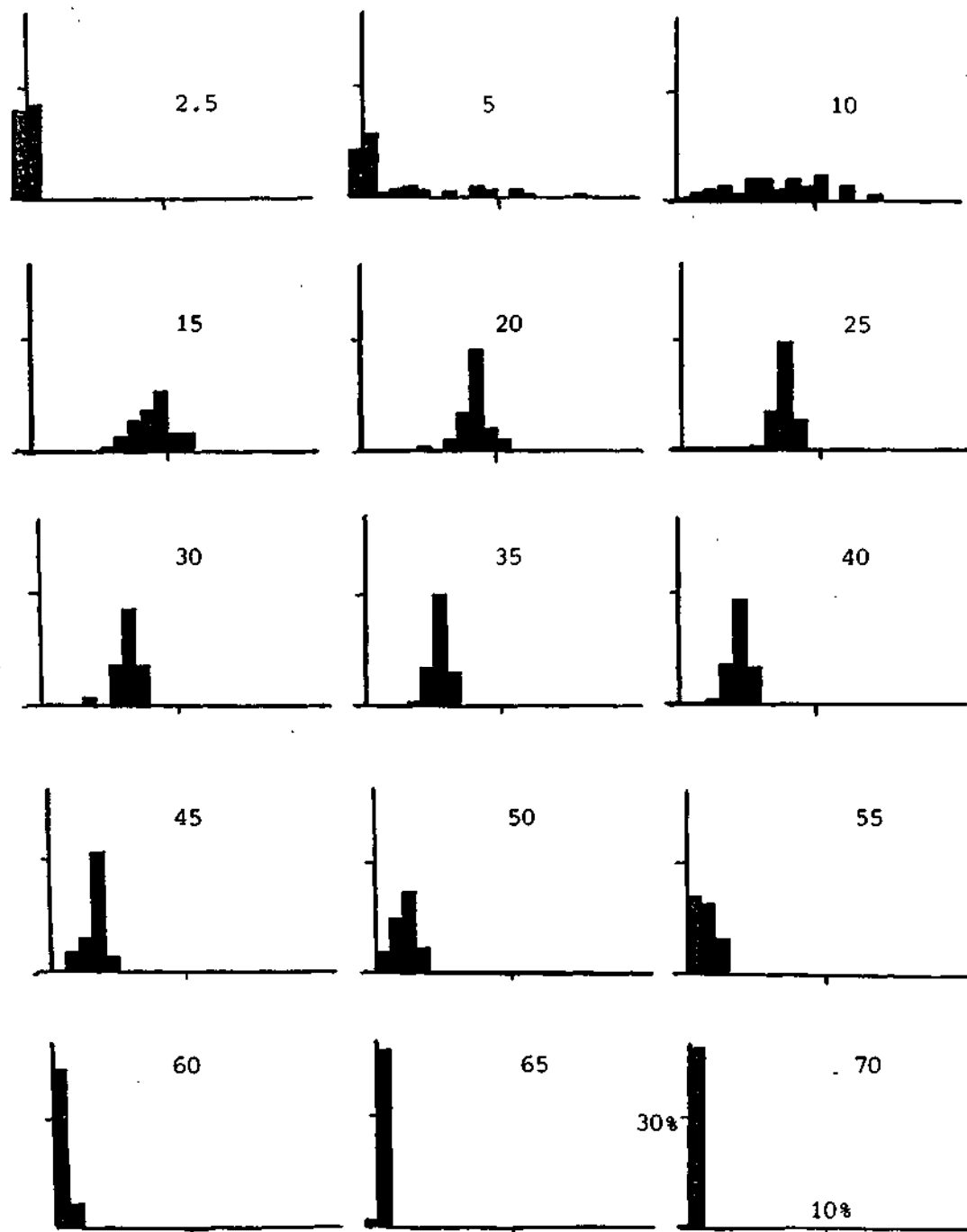
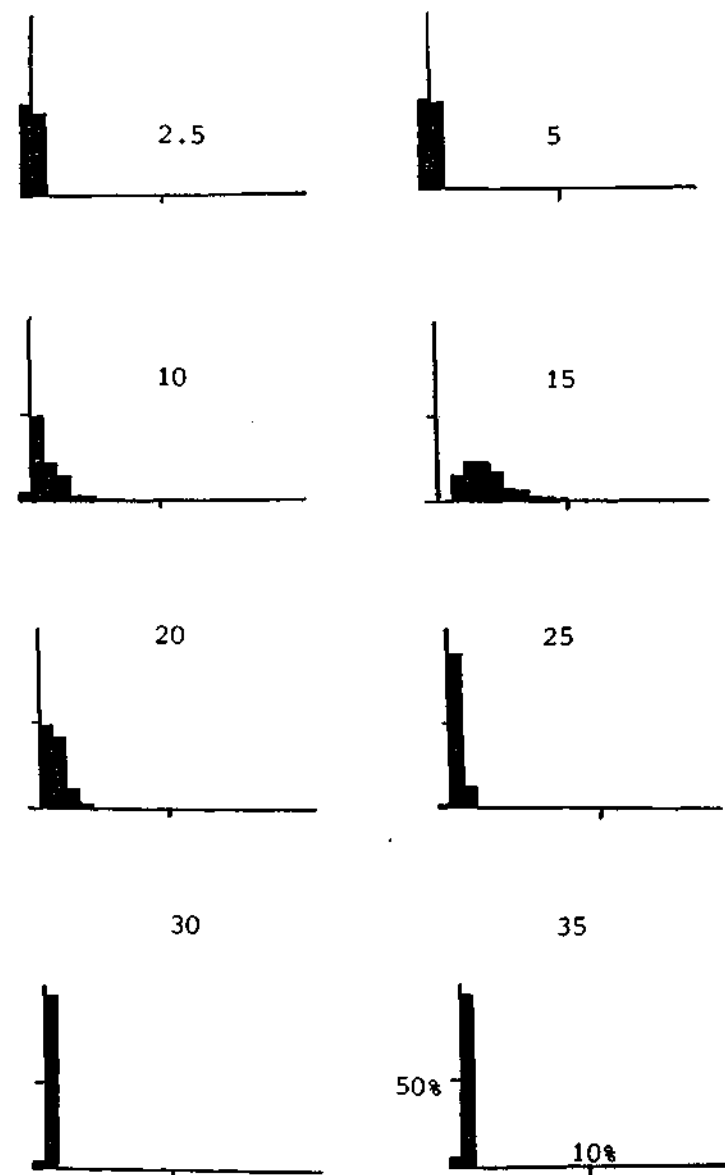


Figure 28 Plot of  $s^2$  against  $m$  for data with  $Ri = 10$  taken at station  $0.7m$  downwind and  $0.004m$  from the wind-tunnel floor. The figures indicate values of  $\tau = Ut/H$ ; the origin is approached as  $\tau$  increases.



(a)  $Ri = 10$ ; 0.7m downwind,  $z = 0.004m$



(b)  $Ri = 0$ ; 0.7m downwind,  $z = 0.004m$

Figure 29 Two typical histograms. The number on each diagram is the value of  $\tau = Ut/H$ , the abscissa is concentration as a percentage and the ordinate is relative frequency as a percentage. (Scale on last diagram in each series.)

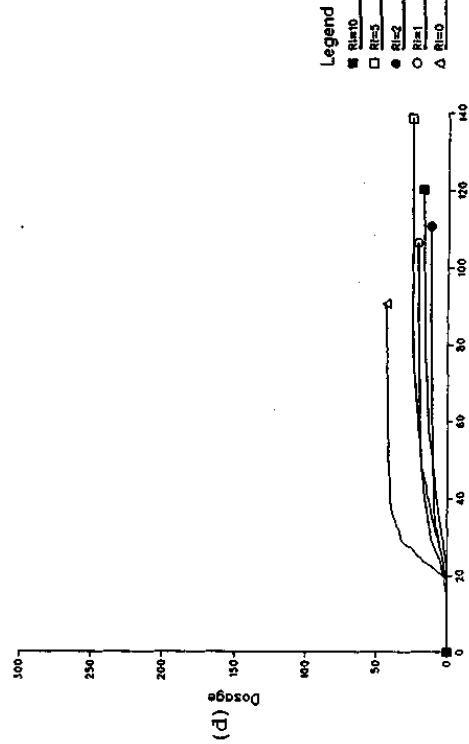
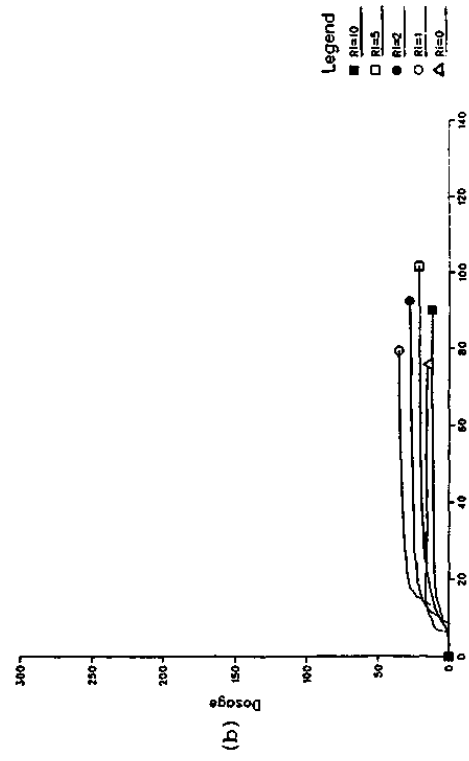
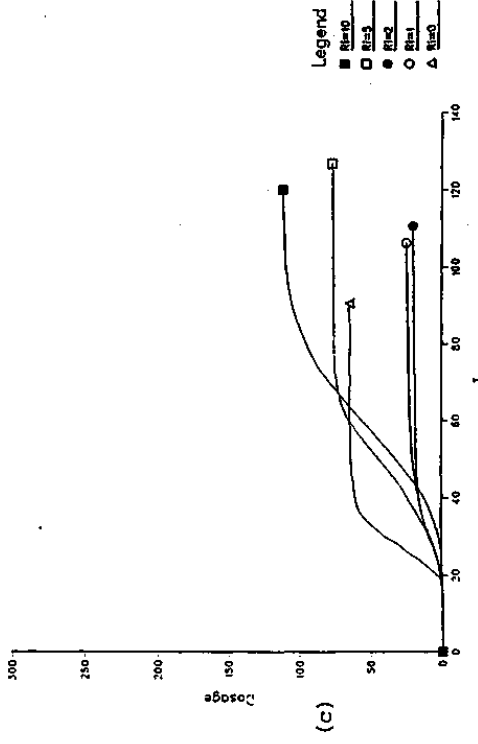
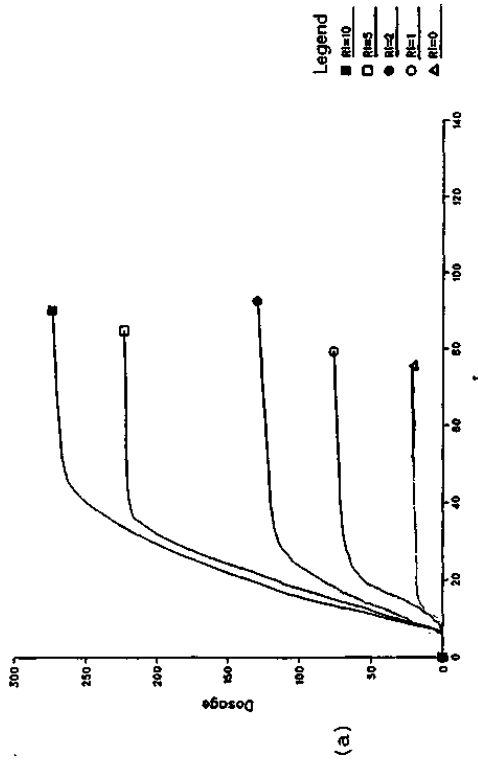


Figure 30 Dosage plots taken at (a)  $x = 0.7m, z = 0.004m$ ; (b)  $x = 0.7m, z = 0.024m$ ; (c)  $x = 2m, z = 0.004m$ ; (d)  $x = 2m, z = 0.024m$ .

**NOT TO BE  
REMOVED**  
FROM THE LIBRARY

**XB 2321432 5**

